Dispersion Stability And Tribological Properties of Covalently Modified Graphene As A Lubricating Oil Additive

Mingyue Wang (mingyuewang61@163.com)
Guangxi University of Science and Technology
Ming Zhou
Guangxi University of Science and Technology
Shengli You
Guangxi University of Science and Technology
Xin Chen
Guangxi University of Science and Technology
Youtang Mo
Guangxi University of Science and Technology
Ziyan Liu
Guangxi University of Science and Technology

Research Article

Keywords: graphene, base oil, lubricant additive, dispersion stability, anti-friction

Posted Date: July 13th, 2021

DOI: https://doi.org/10.21203/rs.3.rs-645776/v1

Dispersion Stability and Tribological Properties of Covalently Modified Graphene as a Lubricating Oil Additive

Mingyue Wang[1,2,3], Ming Zhou[*1,2,3], Shengli You[1,2,3], Xin Chen[1,2,3], Youtang Mo[1,2,3], Ziyan Liu[1,2,3]

1 School of Mechanical and Transportation Engineering, Guangxi University of Science and Technology, Liuzhou 545006, China

2 Guangxi Earthmoving Machinery Collaborative Innovation Center, Liuzhou 545006, China

3 Guangxi Key Laboratory of Automobile Components and Vehicle Technology, Guangxi University of Science and Technology, Liuzhou 545000, China

* E-mail: zhoum03@163.com

Abstract

Graphene has excellent mechanical properties with a low coefficient of friction and wear resistance and has a wide range of tribological applications. However, the stable dispersion of graphene in lubricating media is challenging. In this study, graphene is processed via covalent modification. A mild oxidation method selectively grafts carboxyl groups on the edge of the graphene sheet, before connecting tertiary alkyl primary amines through amide bonds. The alkyl chain allows graphene to be stably dispersed in hydrocarbon solvents.. FT-IR, XPS, Raman, XRD, SEM, etc. are used to characterize the covalently modified graphene (MG). Dispersion stability experiments showed that MG exhibited stable dispersion in 500N base oil and 15w-40 commercial lubricants, with stability for over 2 months. Tribological test results show that MG in 500N and 15w-40 significantly reduces the friction and wear of steel-steel friction pairs. The stable dispersion of MG in lubricating oil enables the formation of a stable chemical reaction film and graphene physical deposition film during the friction, protects the worn surface, and reduces direct contact, thereby significantly reducing friction and wear.

Keywords: graphene; base oil; lubricant additive; dispersion stability; anti-friction

1. Introduction

In recent years, graphene has received extensive attention owing to its excellent

electrical[1–3], thermal[4,5], mechanical[6,7], electrochemical[8,9], and optical properties[10]. Graphene has also attracted great attention in the field of lubrication owing to its excellent mechanical properties, coupled with its unique low coefficient of friction and wear resistance[11–13]. Graphene is considered to be one of the most promising and attractive lubricating nanomaterials. It is an excellent candidate material for solid lubricants[14] and lubricant additives, and has great potential in tribological applications[15].

Although graphene can significantly improve the tribological properties of lubricating oil, it agglomerates easily; thus, its dispersion stability in lubricating oil is poor, resulting in aggregation and precipitation, which is not conducive to the further application of graphene[16]. Under normal circumstances, graphene is prone to irreversible aggregation and precipitation in lubricating oil, mainly because of the insolubility of graphene itself and the existence of van der Waals forces and π-π stacking between the layers[17–19]. The agglomeration of graphene leads not only to precipitation, but also to the loss of wear resistance and anti-friction ability[20]. Preventing agglomeration is particularly important for graphene applications because their unique properties are associated with individual sheets[21, 22].

Surface modification is currently one of the most effective ways to prevent the agglomeration of graphene in lubricating oil. There are three common surface modification methods: covalent bond modification (chemical modification), non-covalent bond modification (physical modification), and element-doping modification. Compared with the other two methods, the covalent bond surface modification method can produce more stable functionalized graphene. The strong covalent bond structure can improve the dispersion stability of graphene in lubricating oil, and it can also improve the anti-friction and anti-wear properties of functionalized graphene; thus, it has attracted the attention of many researchers. The covalent bond modification of graphene refers to the reactive carbon-carbon double bond, carboxyl group, hydroxyl group, epoxy group, and other oxygen-containing groups on the surface of graphene or graphene oxide (GO) that act as reaction sites, and their covalent bonding with the lipophilic group in the agent to achieve surface

modification [23–26]. The carboxyl group is an oxygen-containing group with high activity, and it reacts more easily with the modifier. Therefore, many reports have used carboxyl groups on GO to react with the amino group of alkyl amine to form an amide bond to graft the oleophilic alkyl group and achieve dispersion stability in hydrocarbon solvents.

Choudhary et al. [27] used different alkyl amines to react with the carboxyl groups of GO to form amide bonds, and prepared alkylated graphene with variable alkyl chain lengths. Its dispersion stability increased with an increase in the solvent chain length, while also improving its anti-friction and anti-wear properties. Mungse et al. [28] reduced GO with hydrazine hydrate, before acidifying it with nitric acid, increasing the number of carboxyl and hydroxyl groups on the edges and surfaces of the obtained GO. The amino group of octadecylamine and the carboxyl group in GO were then reacted at a high temperature to form an amide bond. The modified GO had good dispersibility in lubricating oil and exhibited stability for more than one month. Synthetic sulphur-doped GO can also be grafted with alkylamines to generate amide bonds[29]. The prepared alkylated sulphur-doped GO exhibited excellent dispersibility in PAO4 base oil and 928 lubricating oil, as well as a good anti-wear effect. The wear scar diameters were reduced by 43.2% and 17.2% for modified PAO4 base oil and 928 lubricating oil, respectively.

Paul et al. [30] used the same method to prepare alkylamine-functionalized graphene and dispersed it in commercial engine oil to prepare a stable nano-lubricant. The friction and wear of the steel-steel friction pair was improved by dispersing a small amount of functionalized graphene in the oil. In addition, some studies have shown that the use of mixed amines to covalently modify graphene before combination with an effective dispersant improved the dispersion stability of graphene in base oil[31]. The lubricant also significantly improved the friction and wear of the steel ball-steel friction system. Numerous studies have shown that the use of alkylamines to covalently modify graphene through amide reactions and graft lipophilic groups is one of the most effective methods for improving the dispersion stability of graphene in hydrocarbon solvents. Using this principle to prepare stable

covalently modified graphene (MG) is a relatively important topic for the development of nano-lubricants and has the potential to reduce industrial energy consumption and expand the application range of graphene lubrication.

Therefore, this study follows the above-mentioned ideas and innovatively uses a mild oxidation method to directionally graft carboxyl groups on the edge of a graphene sheet. The carboxyl groups are then combined with tertiary alkyl primary amines (PRIMENE 81-R) that possess high temperature stability and wide temperature fluidity; this reaction is performed to prepare the covalently MG with tertiary alkyl primary amine, which is used as an anti-friction and anti-wear lubricant additive. However, the novelty of this study lies in the use of a mild oxidation method to selectively introduce carboxyl groups on the edges of the graphene sheet and PRIMENE 81-R with many excellent properties as the modified substance. Moreover, the dispersion stability of MG in various base oils and commercial lubricants is studied in detail. In this study, a variety of characterisation techniques are used to characterise the covalently MG to determine the chemical structure, elemental content, morphology, and other properties of the sample. Subsequently, the dispersion stability of covalently MG as a lubricant additive in a variety of base oils and commercial lubricants is studied, and the principle is explored and analysed. Finally, the tribological properties of lubricants with MG are studied and compared with those of pure lubricants. The effects of additive concentration, test load, and sliding frequency on the tribological properties of MG lubricants are discussed.

2. Experimental section

2.1 Materials and synthesis of modified graphene

Graphene was purchased from Guangxi Qinglu New Material Technology Co., Ltd.; concentrated sulfuric acid (H_2SO_4) and concentrated nitric acid (HNO_3) were purchased from Xilong Science Co., Ltd.; butanol was purchased from Fuchen (Tianjin) Chemical Reagent Co., Ltd.; phosphorus pentasulfide was purchased from Shanghai Macleans Biochemical Technology Co., Ltd.; PRIMENE 81-R was purchased from The Dow Chemical Company; anhydrous ethanol was purchased

from Chengdu Clone Chemical Co., Ltd. All reagents were of analytical grade and were used without further purification.

GO was prepared using a mild oxidation method; 1 g of graphene was added to 30 ml concentrated sulfuric acid and 10 ml concentrated nitric acid, stirred evenly, and reacted in a 100 °C oil bath for 9 h. After the reaction, the mixed solution was removed, diluted with deionised water, filtered, and washed with deionised water to a pH of 7. Finally, it was placed in an oven and dried at 60 °C for 24 h to obtain GO.

The second step was to prepare the covalently MG. First, 0.3 g of GO prepared by the above method was added to 0.6 g of phosphorus pentasulfide and 6 g of butanol, mixed well, and reacted at 110 °C and 0.1 MPa for 4 h. After cooling to 40 °C, 6 g of PRIMENE 81-R was added to the mixture and reacted at 200 °C and 0.5 MPa for 3 h. After the reaction, the mixture was cooled to room temperature, filtered, and washed thoroughly with absolute ethanol. Finally, it was placed in an oven and dried at 60 °C for 24 h to obtain a black powder: MG.

2.2 Preparation of lubricants

Four sets of lubricants were prepared:

(1) MG was dispersed in PAO6, Shell 420 (Q420), 500N, and 150N base oils at a concentration of 0.01%; these were denoted as MG+PAO6, MG+Q420, MG+500N, and MG+150N, respectively.

(2) Graphene and MG were dispersed in 500N and 150N, respectively, at a concentration of 0.01%; these were denoted as GN+500N and MG+150N, respectively.

(3) MG was dispersed in PAO6, Q420, 500N, and 150N at a concentration of 0.05%, marked as MG(0.05%)+PAO6, MG(0.05%)+Q420, MG(0.05%)+500N, and MG(0.05%)+150N, respectively.

(4) Graphene and MG were dispersed in a commercial lubricant (15w-40) at a concentration of 0.05% and were marked as GN(0.05%)+15w-40 and MG(0.05%)+15w-40, respectively.

Preparation of these lubricants involved ultrasonic dispersion at 35 °C and 300

W for 1 h; no surfactant was used during dispersion.

2.3 Characterization of graphene oxide and modified graphene

The phases, structures, elements, and morphologies of GO and MG were analysed using standard characterisation techniques. Fourier transform infrared (FT-IR) spectroscopy was performed using a PerkinElmer FT-IR spectrometer in Germany, with potassium bromide (KBr) particles as the sample matrix and a scanning wavenumber range of 4000–450 cm^{-1}; the resolution was 4 cm^{-1}. X-ray photoelectron spectrometry (XPS) was done using a Shimadzu Kratos AXIS Ultra DLD XPS. Raman spectroscopy (Raman) detection of the sample was carried out on a Horiba XploRA Raman spectrometer (Japan) with a grating of 1200 nm and a laser length of 532 nm. The scanning Raman shift range was 1000–3000 cm^{-1}. Using a Bruker D8 advanced diffractometer at 40 kV and 40 mA, the sample was subjected to X-ray powder diffraction (XRD) analysis with Cu Kα radiation (λ = 0.15418 nm), and diffraction data at 2θ angles between 10° and 60° were recorded (step angle: 0.02°, step time: 1 s). The morphology of the samples was analysed using a Carl Zeiss SIGMA300 (Germany) scanning electron microscope (SEM).

2.4 Characterization of dispersion stability of modified graphene in lubricants

The dispersion stability of the four MG lubricants was determined using a UV-Vis spectrometer (UV-Vis). Using four pure base oils as a reference, the concentration of MG dispersed in the lubricating oils was monitored to observe the dispersion stability of MG in the oils. According to the Beer-Lambert law, absorbance has a linear relationship with concentration, so a linear standard curve was drawn. Subsequently, the supernatant was scanned at different time intervals to determine its concentration and to evaluate its dispersion stability. The molecular structures of the base oils were analysed using gas chromatography-mass spectrometry (GC-MS). By analysing the molecular structure of the base oil and MG, principle analysis of the dispersion stability of MG in different base oils was carried out.

2.5 Tribological characterization of lubricants

The tribological properties of the MG lubricating oils were studied using a UMT-TriboLab (USA)—a multifunctional ball-plate friction and wear tester and a Shunmao four-ball friction and wear tester (China). First, the UMT-TriboLab was used to conduct friction tests on 500N base oil with MG, and three parameters were studied. First, MG concentrations of 0%, 0.02%, 0.03%, 0.04%, 0.05% were tested with a load of 180 N and reciprocating frequency of 5 Hz. Second, five different loads were set (50, 100, 150, 180, and 230 N) with an MG content of 0.03% and a reciprocating frequency of 5 Hz. Finally, five reciprocating frequencies (1, 3, 5, 7, and 9 Hz) were tested with an MG content of 0.03% and a load of 180 N. For all tests, the following conditions were used: 6 mm reciprocating stroke, 20 min time, and 6 mm ball diameter. After the tests, the friction coefficient and wear scar size were obtained to evaluate the tribological properties of the lubricant.

A four-ball friction and wear tester was then used to conduct tribological experiments on MG lubricating oil prepared by adding MG to 500N base oil and 15w-40 commercial lubricating oil at varying concentrations. All tests were carried out at 25℃ under a load of 392 N and a speed of 1200 rpm. After the test, the friction coefficient and wear scar diameter were obtained to evaluate the tribological properties of the lubricant.

3. Results and discussion

3.1 Chemical and structural analysis of GO and MG

Owing to the different cohesive energies of graphene and the dispersion medium, they are immiscible with most organic solvents and hydrocarbons[32]. However, for effective lubrication, the graphene flakes should be completely dispersed in the lubricating oil. Generally, graphene is stable and has no chemical activity in most organic solvents. Therefore, to modify graphene using covalent bonds, active sites such as oxygen-containing groups must be introduced to the graphene sheet and connect with the modified groups to promote their dispersion in the lubricating oil. In many studies, the improved Hummer's method has been used to prepare GO, but this

method uses a strong oxidant that destroys the atomic structure of graphene while introducing oxygen-containing functional groups. Moreover, the MG prepared using GO has more oxygen-containing functional groups, and the shear resistance between the layers of the friction contact interface is relatively high, meaning the anti-friction and anti-wear effects are poor. Suk et al. [33] used atomic force microscopy to reveal that the excessive presence of oxygen-containing functional groups in GO impaired its mechanical properties, and the effective Young's modulus was lower than that of graphene. In this study, a mild oxidation method using a mixture of sulfuric acid and nitric acid was used to selectively introduce carboxyl groups as active sites at the edges and defects of the graphene sheet to preserve as much of the atomic structure of graphene as possible. The use of this method was inspired by research by Wepasnick et al. on the oxidation of CNTs [34]. However, using the same oxidation method for graphene sheets and carbon nanotubes will yield different results, so GO-1 was prepared according to another method mentioned in the literature for comparison. Graphene oxide with concentrated nitric acid is used alone to prepare GO-1.

The carboxyl group introduced onto the graphene sheet was used for covalent bond modification; the carboxyl group was attached to PRIMENE 81-R through an amide bond, and the alkyl chain at the other end of PRIMENE 81-R was used to stably suspend the MG in the lubricating oil. Moreover, PRIMENE 81-R itself has high solubility in hydrocarbon solvents, and its derivatives can also have good oil solubility. It also has good stability and oxidation resistance at high temperatures and can resist high temperatures and high shear forces during friction. In addition, PRIMENE 81-R is a liquid over a wide temperature range and has excellent fluidity. The alkyl amine commonly used in previous studies, octadecylamine, is a waxy solid. In contrast, PRIMENE 81-R is more convenient for the reaction and post-processing of the samples.

Through FT-IR, XPS, Raman, and XRD analyses, the chemical and structural changes that occurred during the preparation of MG with GO as the precursor were comprehensively monitored. Figure 1 shows the infrared spectra of the GO and MG. GO exhibited strong vibration peaks at 1717, 1588, 1386, 1223, and 1056 cm^{-1}.

Among them, the peak at 1717 cm^{-1} is due to the carboxyl group causing C=O stretching, 1588 cm^{-1} is C=C stretching with an unoxidized carbon structure, 1386 cm^{-1} is the O-H bending vibration, 1223 cm^{-1} is C-O-C stretching caused by phenols, ethers, and epoxy groups, and 1056 cm^{-1} is C-O stretching caused by the hydroxyl group. These characteristic vibration peaks reveal the presence of oxygen-containing functional groups, such as carboxyls, hydroxyls, epoxys, carbonyls, phenols, and ethers. Over the years, various structural models of GO have been studied, and most of the hydroxyl and epoxy functional groups are located on the base plane, while the carboxyl groups are located at the edge[35]. The presence of carboxyl groups at 1717 cm^{-1} causes C=O stretching, which indicates that mild oxidation using a mixture of sulfuric acid and nitric acid can selectively introduce carboxyl groups at the defect sites of graphene. Subsequently, through a high-temperature reaction, an amide bond is formed and the GO can couple with PRIMENE 81-R. The FT-IR spectrum of MG showed vibration peaks at 1707, 1578, 1400, and 1003 cm^{-1}; 1707 cm^{-1} is the C=O of the amide group, 1578 cm^{-1} is N-H bond and carbon structure C=C stretching, and 1120 cm^{-1} is the stretching vibration of C-N, indicating that PRIMENE 81-R was successfully loaded onto the graphene.

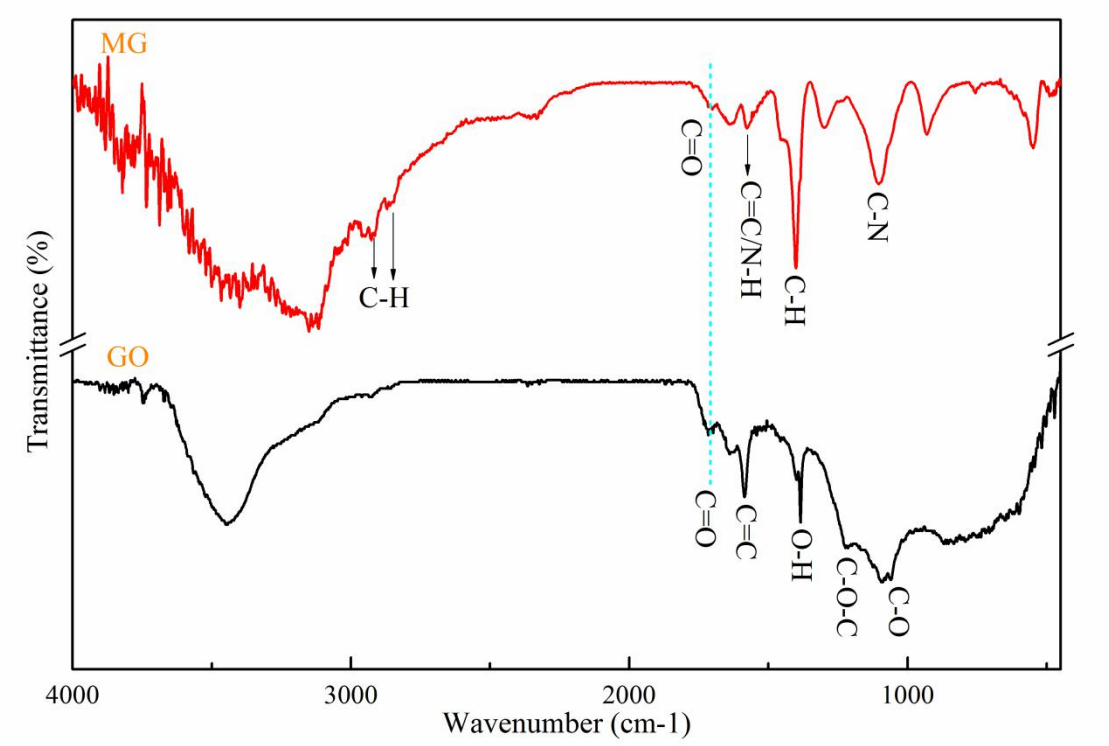

Figure 1. FTIR spectra of GO and MG.

We also attempted to use other oxidants to mildly oxidise graphene. Following the oxidation method of Wepasnick et al. [34], concentrated nitric acid was used to obtain graphene oxide (GO-1). Using concentrated nitric acid and concentrated sulfuric acid 1:3-mixed oxidised graphene (GO) as a comparison, infrared spectroscopy was used to detect their functional groups, and the infrared spectra of the two GOs are shown in Figure 2. It can be seen from the comparison that the biggest difference between the GOs is that the carboxyl group at 1717 cm^{-1} in the GO spectrum causes C=O stretching, while this characteristic peak does not appear in the GO-1 spectrum. This shows that solely using concentrated nitric acid to oxidise graphene cannot selectively introduce carboxyl groups on the edges of graphene. This also proves that the mild oxidation method we explored can replace the use of strong oxidants to achieve the purpose of generating carboxyl groups on the edge of the graphene sheet. Therefore, oxidation was performed using a 1:3 mix of concentrated nitric acid and concentrated sulfuric acid for all other experiments.

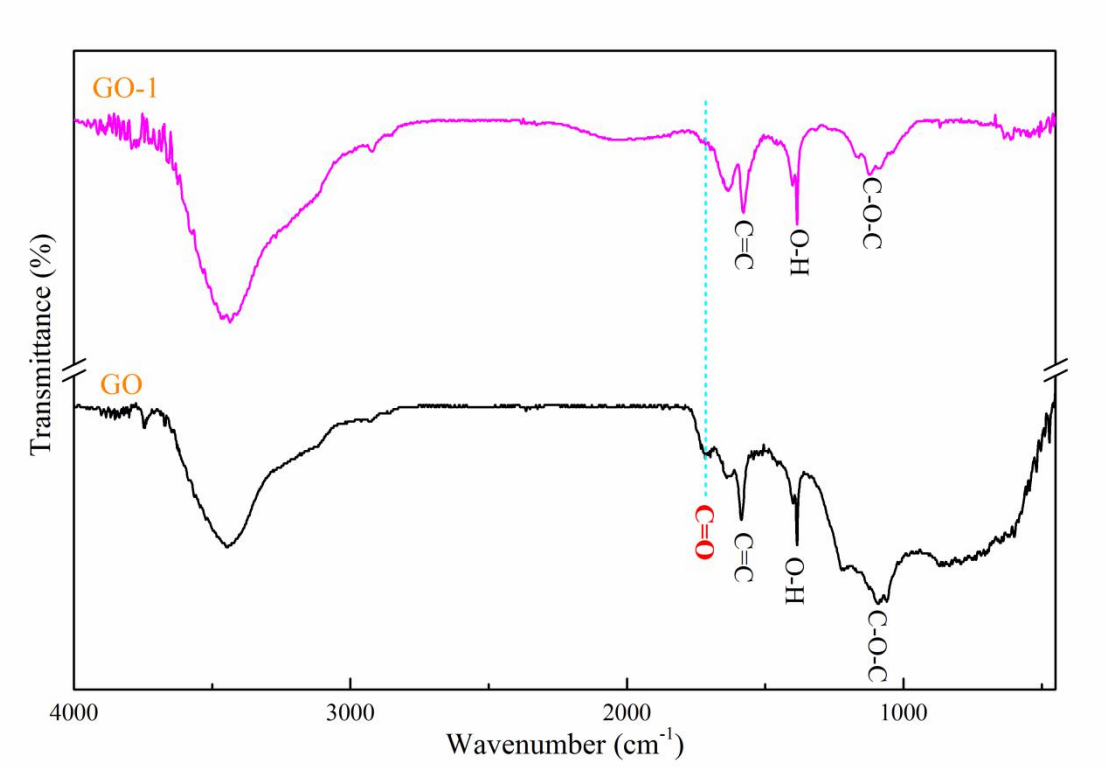

Figure 2. FTIR spectra of GO-1 and GO.

Subsequently, XPS analysis was performed on GO and MG to observe the

further chemical changes. Figure 3a and b shows the XPS spectra of GO and MG, respectively. The XPS spectrum of GO exhibits peaks corresponding to C1s and O1s. The atomic contents of C and O were also detected, which were 91.97% and 8.03%, respectively. The XPS spectrum of MG contains three elements, C, O, and N, with atomic contents of 91.86%, 5.91%, and 2.23%, respectively. Figure 2b also shows the C1s spectrum of MG, which appears as a single peak and a small tail at a higher binding energy. A very strong peak associated with C=C/C−C (284.5 eV) reveals clear signs of PRIMENE 81-R loading on the GO film. The alkyl chain of PRIMENE 81-R contributes to the significant increase in the intensity of the C1s peak at 284.5 eV. The C1s spectrum of MG shows that at 285.6 and 288.0 eV, there are two chemical shift components moving towards a higher binding energy, which are attributed to the amine/hydroxyl group (CN/C-O) and amide/carbonyl group (CONH-R/C=O) respectively. The N1s XPS spectrum at 400 eV (Figure 2b) confirms the presence of amide groups in MG. Elemental analysis of all samples showed that the GO prepared as an intermediate product did not contain N. Therefore, the N content in MG confirms the grafting of PRIMENE 81-R onto GO. This also proved the feasibility of PRIMENE 81-R grafting onto graphene sheets, and found a new type of alkylamine that is different from the previous studies.

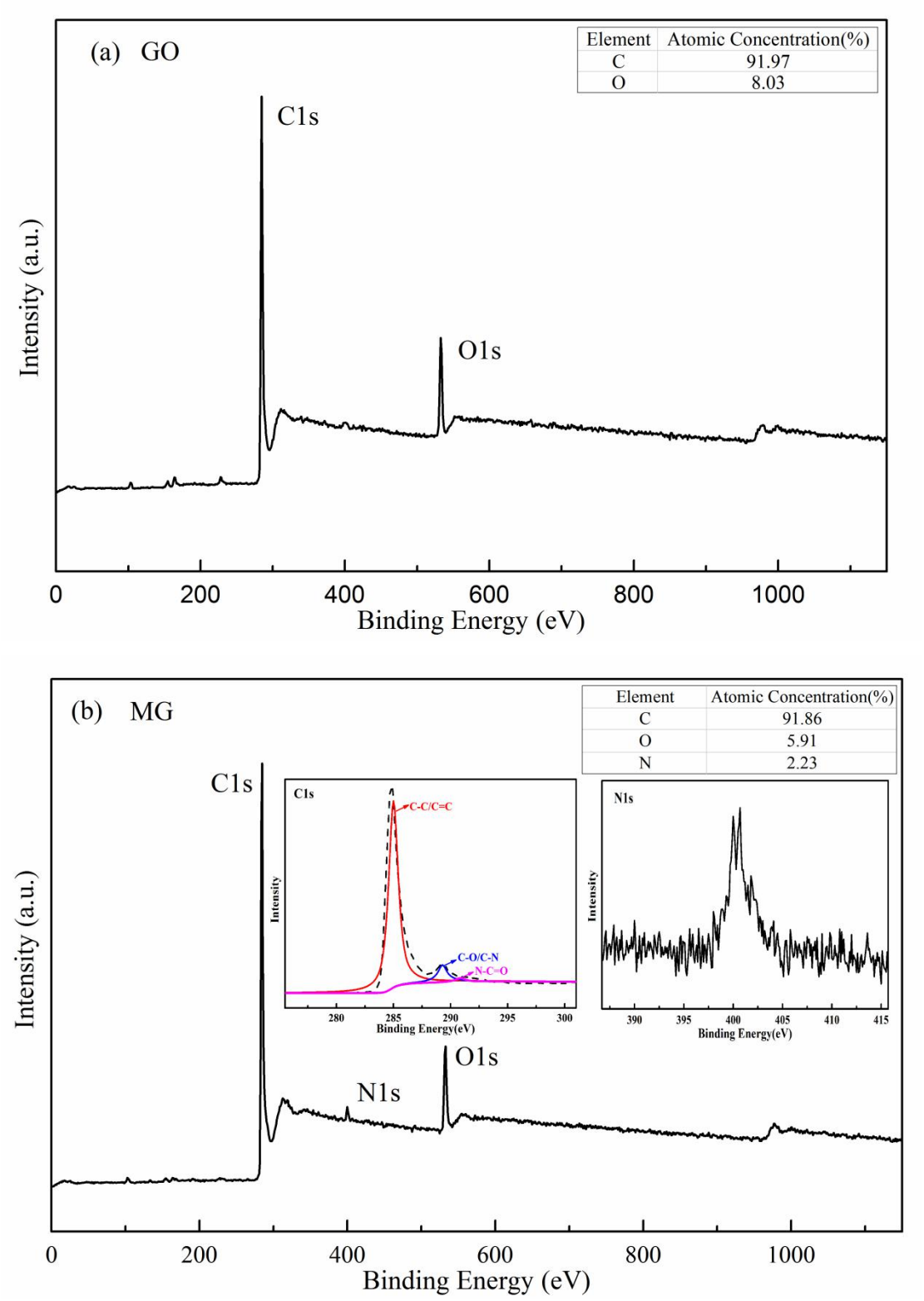

Figure 3. XPS spectra of (a) GO and (b) MG with their C1s and N1s spectra.

Raman spectroscopy is a commonly used non-destructive environmental detection technique for characterising the electronic structure of graphene-based materials. Figure 4 shows the Raman spectra of the GO and MG. The D and G peaks

of GO appear at Raman shifts of 1350 and 1580 cm^{-1}, respectively, and the D and G peaks of MG appear at Raman shifts of 1336 and 1570 cm^{-1}, respectively. The D peak represents the presence of sp^3 hybrid carbon atoms, which is caused by the loss of sp^2 domains due to defects; the G peak represents the stretching of sp^2 carbon atoms. The intensity ratio of the D and G peaks (I_D/I_G) is related to the degree of disorder of graphene. The I_D/I_G values of GO and MG are 0.18 and 0.74, respectively. The I_D/I_G value of MG is larger than that of GO, which is caused by the formation of more sp^3 hybrid carbon atoms in the sp^2 carbon grid of MG, indicating that the modified groups on the graphene were successfully grafted. This is consistent with the FT-IR and XPS results. In this work, GO and MG powders were characterised by XRD, and the structural changes that occurred during the chemical modification of GO; specifically, the changes in the distance between layers, a key parameter of the lubrication angle, were analysed. As shown in Figure 5, the diffraction peak of GO was at $2\theta = 24.3°$, and the diffraction peak of MG was at $2\theta = 26.3°$. According to the Bragg formula ($2d\sin\theta = n\lambda$, where d is interlayer spacing, n is the diffraction order, and λ is wavelength) d = 0.19250 and 0.17385 nm for GO and MG, respectively. The oxygen-containing functional groups on the GO substrate cause distortion of the sp^2 carbon network, weakening the van der Waals interaction between the GO layers, and causing the layer spacing to increase. However, the interlayer spacing of GO does not increase significantly; this may be because the mild oxidation method used mostly generates carboxyl groups at the edge of the graphene sheet, meaning there are not many oxygen-containing functional groups on the base surface. This shows that the mild oxidation method we used did graft carboxyl groups on the edge of the graphene sheet, and inhibited the generation of oxygen-containing functional groups on the base surface. Compared with the use of strong oxidants in previous studies, this is indeed a more excellent and feasible method. The shift of the MG diffraction peaks and the reduction of interlayer spacing are caused by the removal of oxygen-containing functional groups and the recovery of carbon content in the MG sheet, indicating that PRIMENE 81-R can reduce GO in addition to grafting onto the surface of GO.

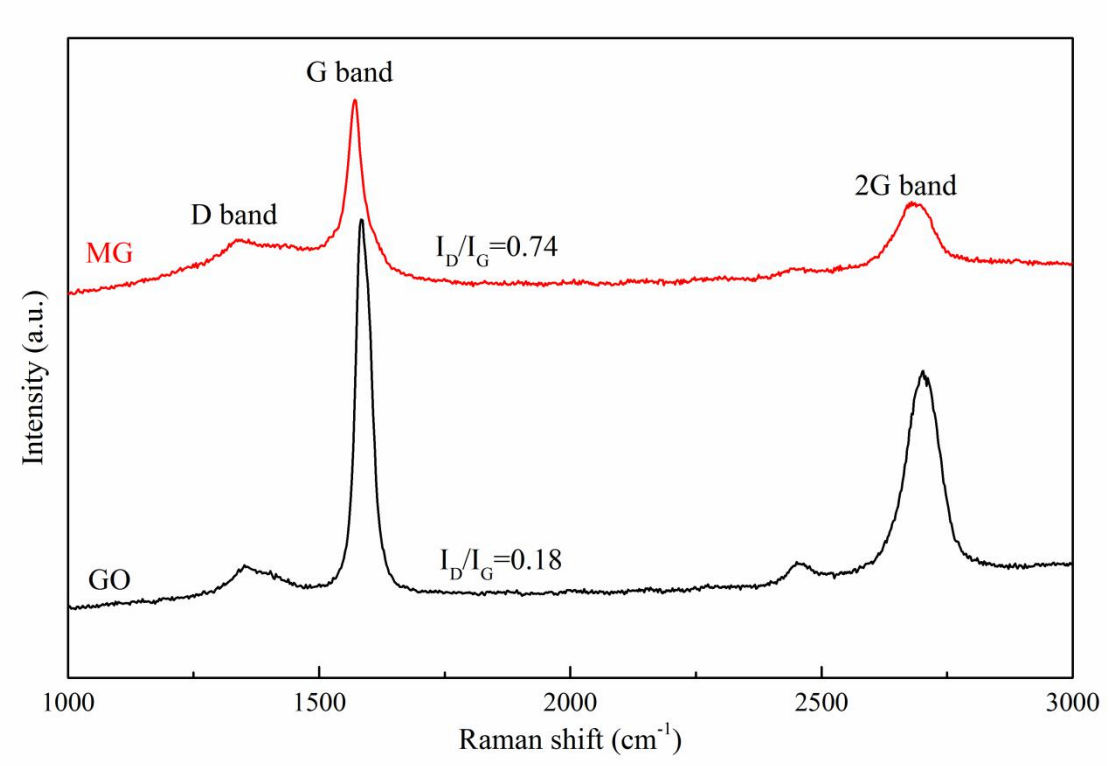

Figure 4. Raman spectra of GO and MG

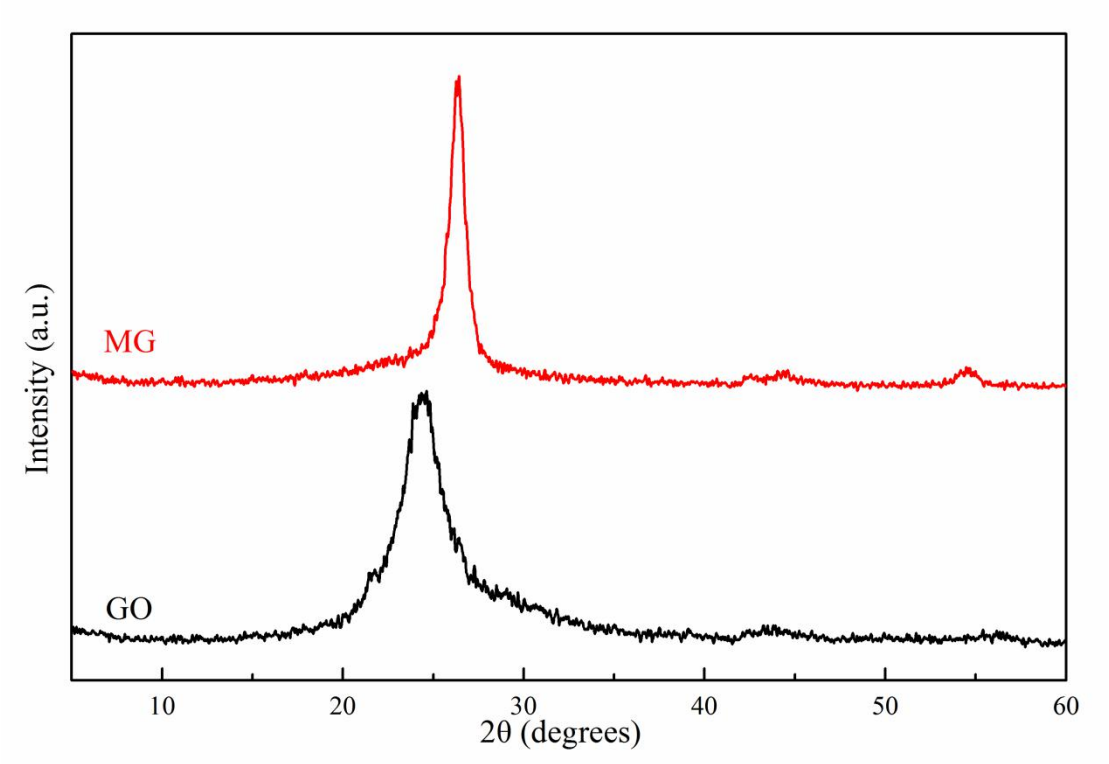

Figure 5. XRD patterns of GO and MG powder.

In this study, SEM was used to analyse the morphologies of GO and MG. Figure 6(a) and (b) shows SEM images of GO and MG, respectively. In the figure, GO is a

flat sheet with slightly broken edges, exhibiting a relatively complete graphite-like structure with some overlap and curl. However, the GO surface has no visible defects, which is the result of mild oxidation. It was mentioned earlier that the carboxyl groups were mainly distributed on the edge of the GO. Therefore, the directional grafting of carboxyl groups does not damage the sheet structure of graphene, and the GO has a relatively complete conjugated structure. This has a more significant effect on the subsequent MG as a lubricant additive; a large number of oxygen-containing functional groups in the MG increases the shear resistance between the layers of the friction contact interface, and the anti-friction and anti-wear effects are poor. Moreover, hydrogen bonding between oxygen-containing functional groups may facilitate the agglomeration of graphene. Figure 6(b) shows the SEM topography of the MG. It can be seen from the figure that the MG layer has clear wrinkles and curls than the GO layer. The wrinkles and folded edges of the MG nanostructure may carry alkyl chains, which play a vital role in their effective dispersion in organic solvents. This also confirms the successful grafting of PRIMENE 81-R on graphene sheets, which is consistent with the FT-IR, XPS, Raman, and XRD results.

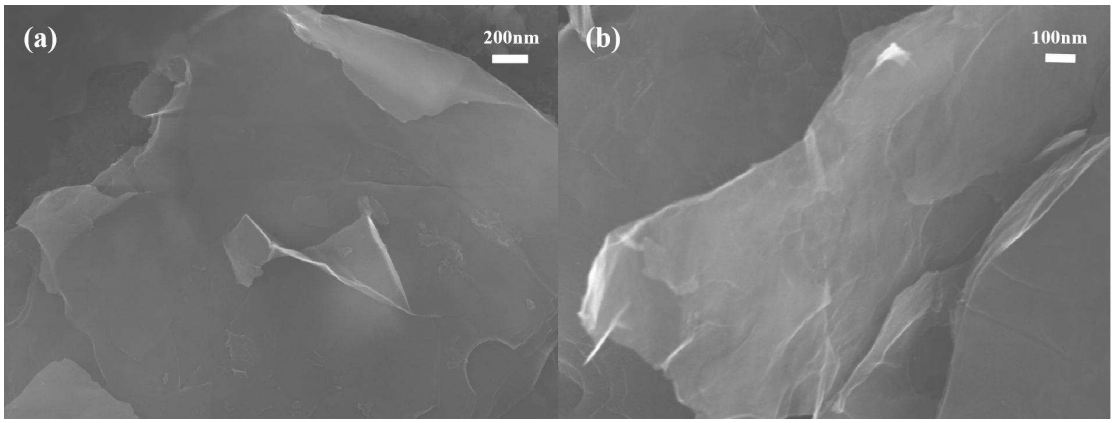

Figure 6. SEM images of (a) GO and (b) MG

3.2 Analysis of dispersion stability of modified graphene in lubricants

The dispersion stability of the MG lubricants was studied using a UV-vis spectrophotometer. According to the Beer-Lambert law, the concentration of a dispersion is directly proportional to its absorbance. After a certain time interval, the

absorbances of the four groups of prepared lubricating oils were collected, and the concentration changes were obtained through their respective concentration standard curves.

First, dispersion stability testing was performed on the first group of lubricants. We collected the wavelength curves of MG in four base oils: PAO6, Q420, 500N, and 150N, as shown in Figure 7(a). Next, 303, 232, 250, and 329 nm were taken as fixed points, and the concentration standard curve of MG in the four base oils was drawn, as shown in Figure 7(b). Figure 8 shows the concentration of MG in the four base oils over time. Measurements were recorded every 24 h for the first 15 days to obtain the concentration value; measurements were then taken every 5 days to evaluate the stability over 60 days. In the first 10 days, the concentration of MG in the four base oils continued to decrease, which was caused by the sedimentation of large MG particles. The concentration of MG in 500N remained stable from the 10th day, PAO6 and Q420 stabilised on the 15th day, and 150N was stable from the 20th day.

For all base oils, MG created a stable and uniform system that could be maintained for approximately two months. This fully demonstrates the successful grafting of PRIMENE 81-R on graphene, and reflects its excellent performance in improving the dispersion stability of graphene. It is a new and highly feasible modified substance. However, the stable concentrations of MG in the base oils varied significantly. From the figure, the stable concentration value of MG in 500N is the highest, followed by PAO6, Q420, and 150N; the stable concentrations of the latter three are similar. This phenomenon may be caused by the different binding energies of the PRIMENE 81-R carbon chain grafted on the MG and the four base oils, as well as the different physical and chemical properties of the base oils.

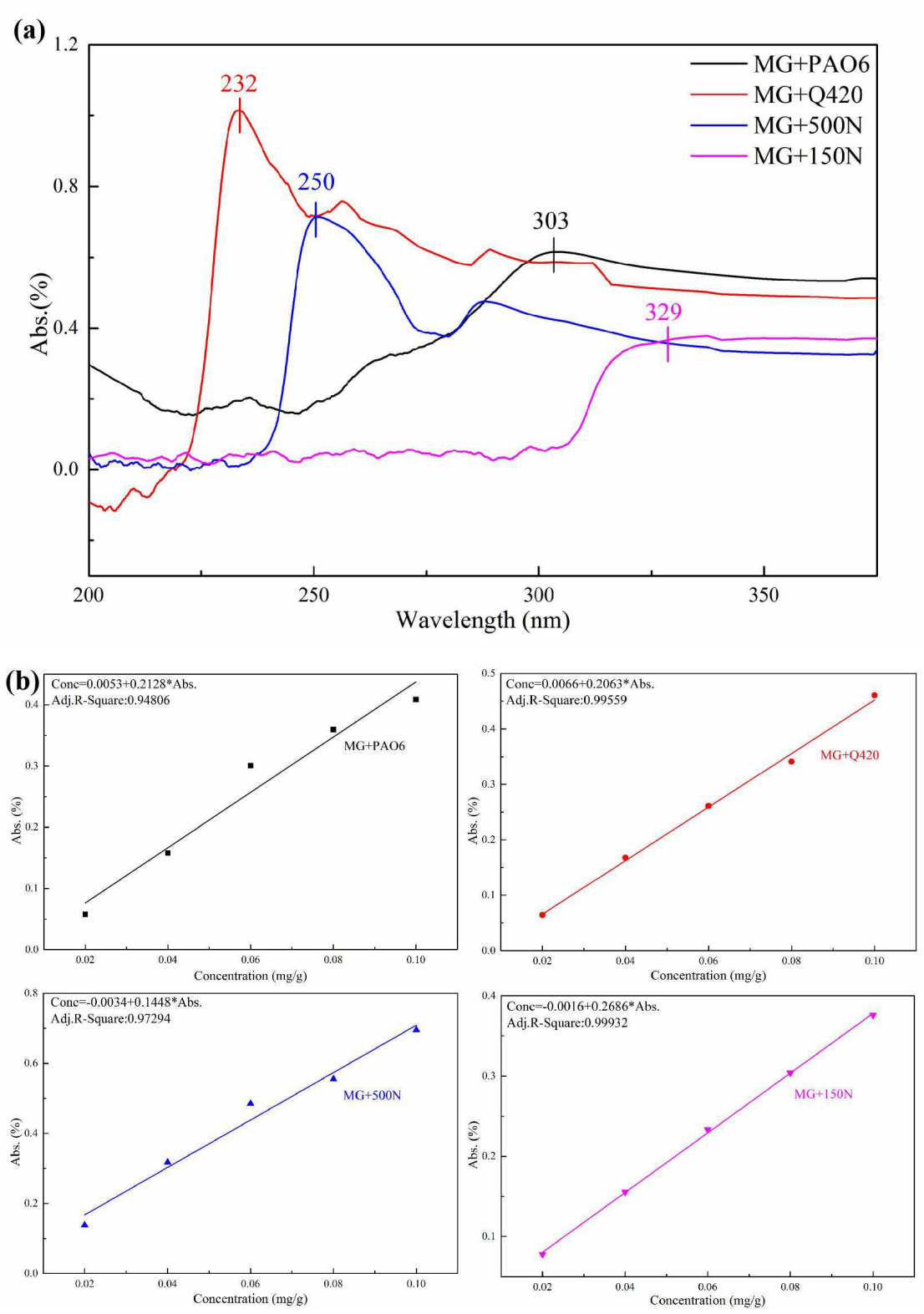

Figure 7. (a) Wavelength diagrams of MG in four base oils; (b) standard curves of MG (0.01% addition) in the base oils

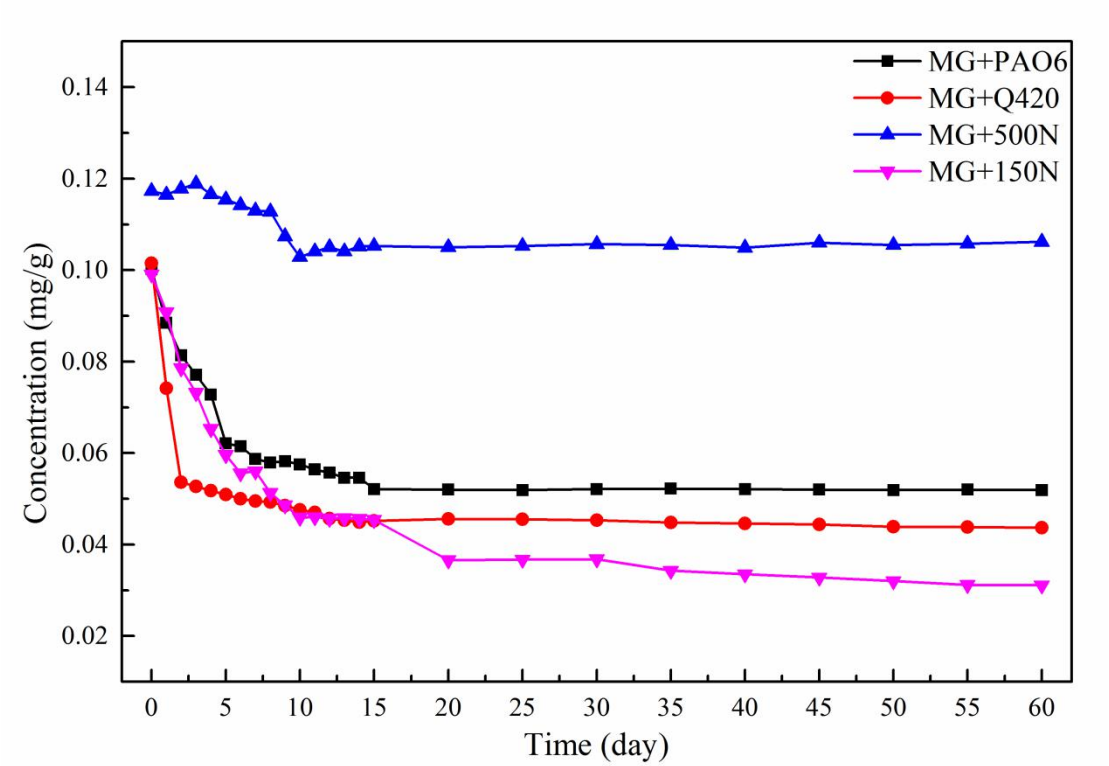

Figure 8. Concentration versus time curves of MG (0.01% addition) in the four base oils

The second set of MG lubricating oil dispersion stability experiments were performed in a similar way. Figure 9 shows the wavelength diagram (a) and standard curve diagram (b) of graphene dispersed in 500N. A standard curve was drawn using 413 nm in the wavelength diagram as a fixed point; this was then used to monitor the concentration changes of graphene and MG in 500N and conduct comparative experiments. Figure 10 shows the time curve of the concentration of graphene and MG (0.01% addition) in 500N. It can clearly be seen from the figure that the concentration of graphene in the 500N continued to decrease over 60 days (0.1 to ~ 0.01 mg/g). In the first 25 days, the concentration decline rate was relatively high; after this, the concentration gradually decreased, and the decline rate also reduced. The rapid decrease in the concentration in the early stage was due to the high content of graphene flakes in the base oil. Owing to the attraction of van der Waals forces, the graphene flakes are attracted to each other, their volume becomes larger, and they gradually settle. In the later stage, the concentration decreases, the spacing between graphene sheets becomes larger, agglomeration reduces, and the sedimentation speed

slows. The concentration of MG in 500N decreased slightly in the first 10 days and remained stable at approximately 0.1 mg/g thereafter. This shows that the dispersion stability of MG in 500N base oil improved significantly compared to graphene. At the same time, it also shows that graphene has been successfully modified, and PRIMENE 81-R has a significant effect in improving the dispersion stability of graphene.

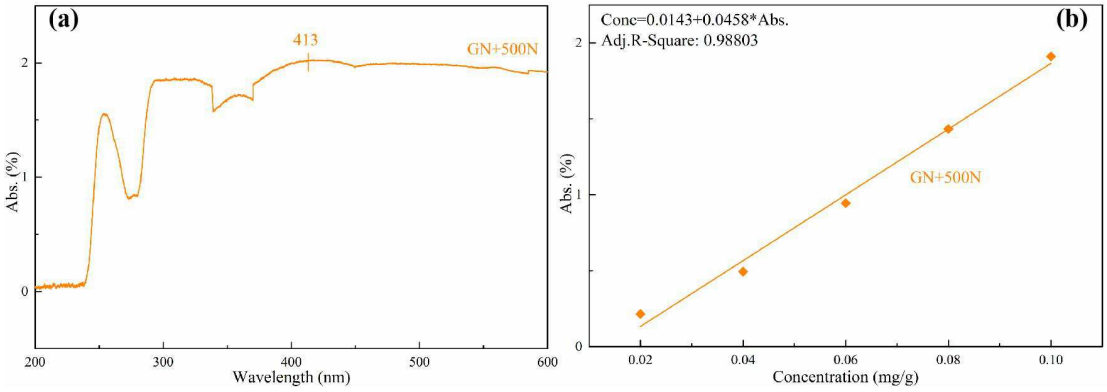

Figure 9. (a) Wavelength diagram and (b) standard curve diagram of GN+500N

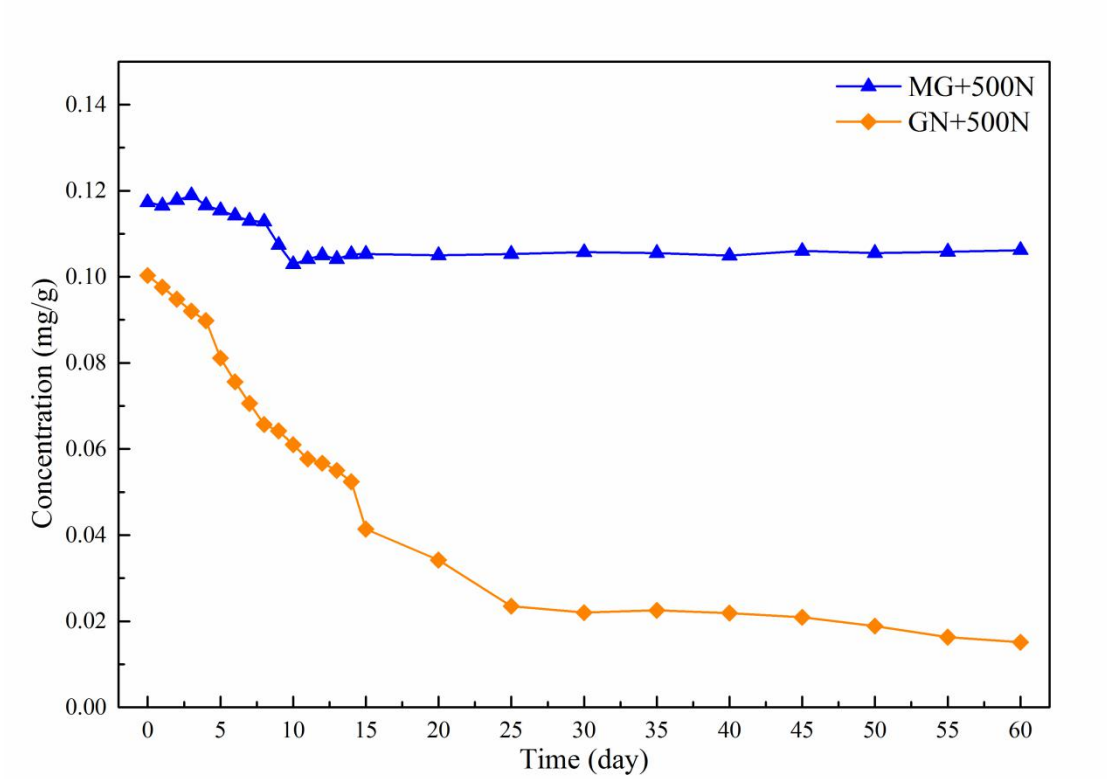

Figure 10. Concentration versus time curves of GN+500N and MG+500N (0.01% addition)

Subsequently, the third group of MG lubricants (MG(0.05%)+PAO6,

MG(0.05%)+Q420, MG(0.05%)+500N, MG(0.05%)+150N) were tested for their dispersion stability. In the first set of experiments, we obtained the wavelength curves of MG in the four base oils, as shown in Figure 7(a). Therefore, 303, 232, 250, and 329 nm were used as fixed points to draw the concentration standard curves of MG (0.05% addition) in the four lubricating oils, as shown in Figure 11. According to the concentration standard curve in Figure 11, the concentration of MG in the four base oils over time with the addition of 0.05% MG was drawn to analyse the stability of its dispersion in lubricating oil, as shown in Figure 12. The same was done every 24 h for the first 15 days, and the concentration of MG in the lubricating oil was recorded. After that, it was tested every five days and recorded for 50 days. It can be seen from the figure that with the addition of 0.05% MG, the best dispersion stability was observed for the 500N base oil.

In the first 35 days, the concentration of MG in 500N base oil gradually decreased from 0.5 to approximately 0.3 mg/g at a consistent rate. From the 35th to the 50th day, the concentration stabilised at 0.3 mg/g. In PAO6, the concentration of MG reduced from 0.5 to approximately 0.064 mg/g in the first 35 days, before stabilising; the concentration was stable at approximately 0.06 mg/g until the 50th day. When 0.05% of MG was added, the stable concentration of MG in PAO6 was similar to that obtained when 0.01% of MG was used; both were approximately 0.064 mg/g. In the first 30 days, the concentration of MG in Q420 continued to decrease from the initial concentration of 0.5 to approximately 0.052 mg/g, and remained stable thereafter. This stable concentration was also similar to that obtained at an addition amount of 0.01%. The dispersion performance of MG in 150N was similar to that of Q420. Its concentration dropped from 0.5 to approximately 0.028 mg/g, which is consistent with that found with the addition of 0.01% MG. Therefore, the dispersion stability of the MG lubricants in this group are similar to those of the first group. That is, MG has the best dispersion stability performance in 500N base oil, and its performance in the other three lubricants was similar. From the third set of experiments, the dispersion and stable concentration of MG in 500N base oil can reach 0.3 mg/g, with a mass ratio is 0.03%. After the addition of MG increases, it can

still be stably dispersed in 500N for at least 50 days. This has a very obvious improvement effect on the dispersion stability of graphene. Compared with previous related studies, there is also a significant improvement.

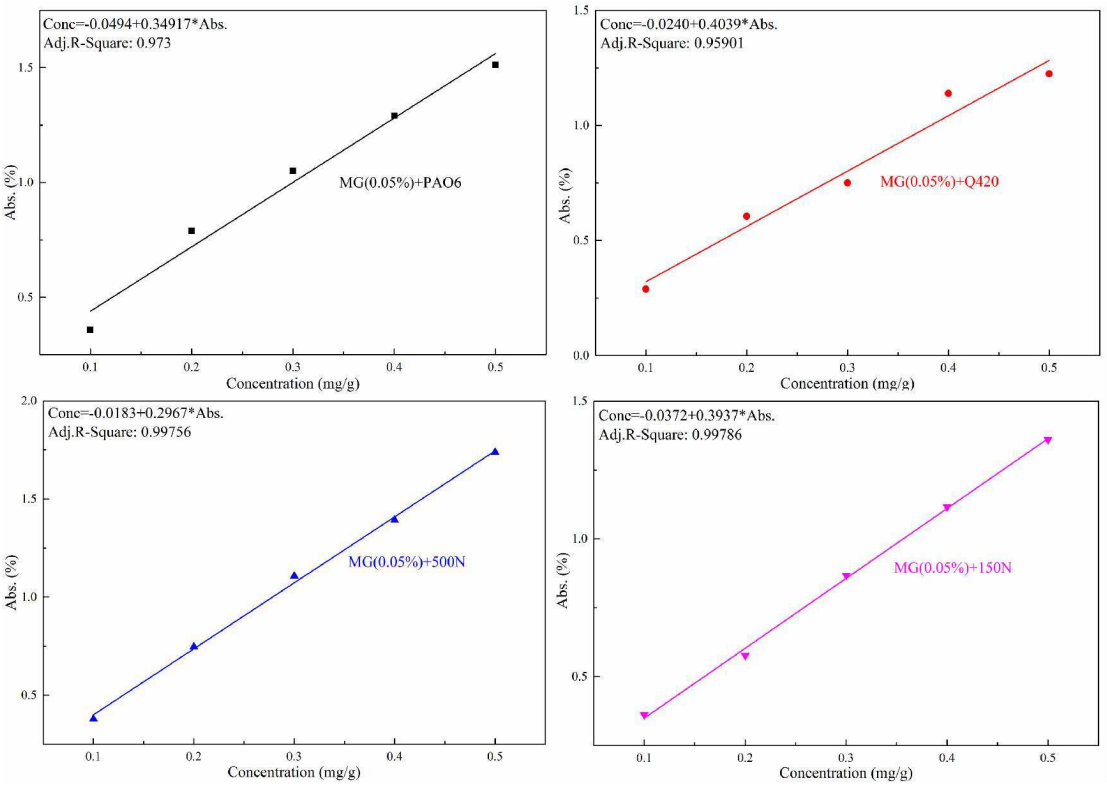

Figure 11. Standard curves of MG (0.05% addition) in four base oils

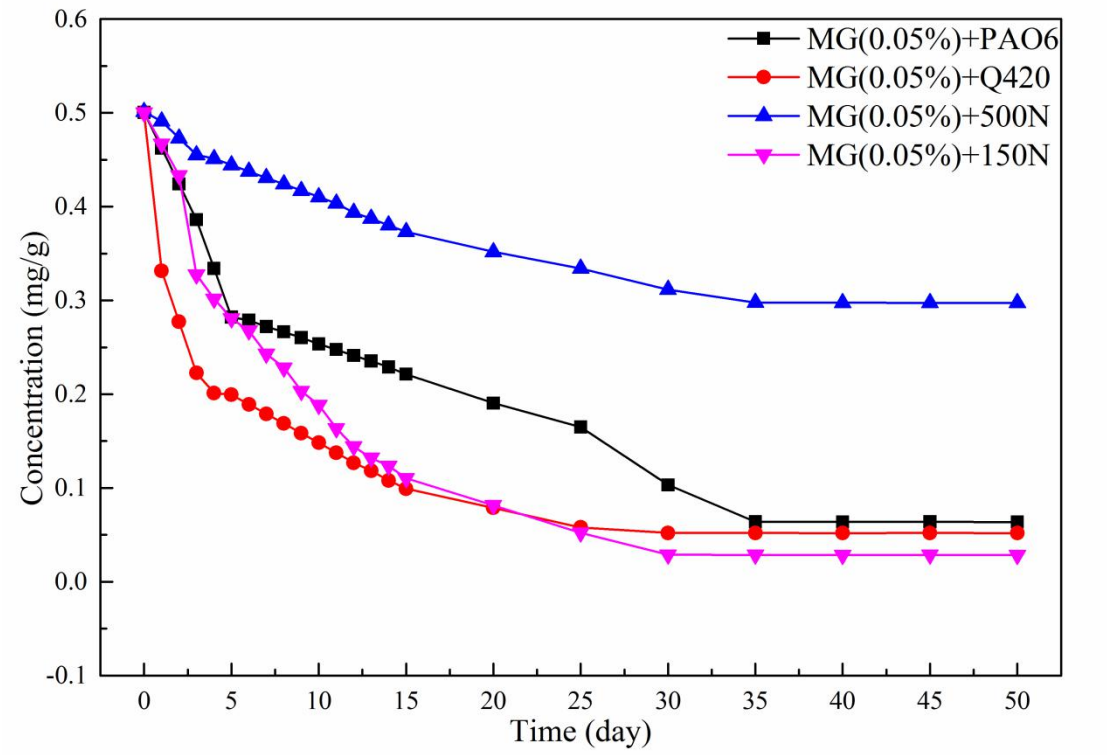

Figure 12. Concentration versus time curves of MG (0.05% addition) in the four base

oils

To test the dispersion stability of MG in commercial lubricants and compare it with the dispersibility of graphene in commercial lubricants, a fourth set of experiments was carried out. Graphene and MG were heated and ultrasonically dispersed in a commercial lubricant (15w-40) at a concentration of 0.05% and denoted as GN(0.05%)+15w-40 and MG(0.05%)+15w-40. According to the experimental method, the wavelength diagrams of graphene and MG dispersed in 15w-40 lubricating oil were obtained, as shown in Figure 13 (a) and (b), respectively. The standard curves of graphene and MG dispersed in 15w-40 lubricating oil with 500 nm as a fixed point were drawn, as shown in Figure 13 (c) and (d). According to the standard curve, the concentration changes of graphene and MG in 15w-40 lubricating oil were monitored, and a curve was drawn, as shown in Figure 14.

It can be seen from the figure that within 60 days, the concentration of graphene in 15w-40 lubricants decreased continuously from 0.5 to 0.035 mg/g. In the early stage, the concentration of graphene nanosheets is large because the van der Waals forces between them cause attraction and settling. In the later stage, the concentration decreases and agglomeration weakens, so the rate of concentration decrease reduces. In general, without dispersant or modification treatment, graphene nanosheets cannot exist stably in lubricating oil. The dispersion performance of MG in 15w-40 lubricants was better than that of graphene. In the first 40 days, the initial concentration of 0.5 mg/g also continued to decrease, but after 40 days, the concentration began to stabilise at approximately 0.2 mg/g. The decrease in the concentration in the early stage may be caused by the sedimentation of the large area of MG nanoplatelets suspended in the lubricating oil, but it can still be stabilised at a higher concentration range in the later stage. These experimental results show that MG has better dispersion stability than graphene in commercial 15w-40 lubricants. MG is not only stable in dispersion in 500N base oil, but also in commercial lubricants. It shows that the method we use to modify graphene is very excellent and has great feasibility.

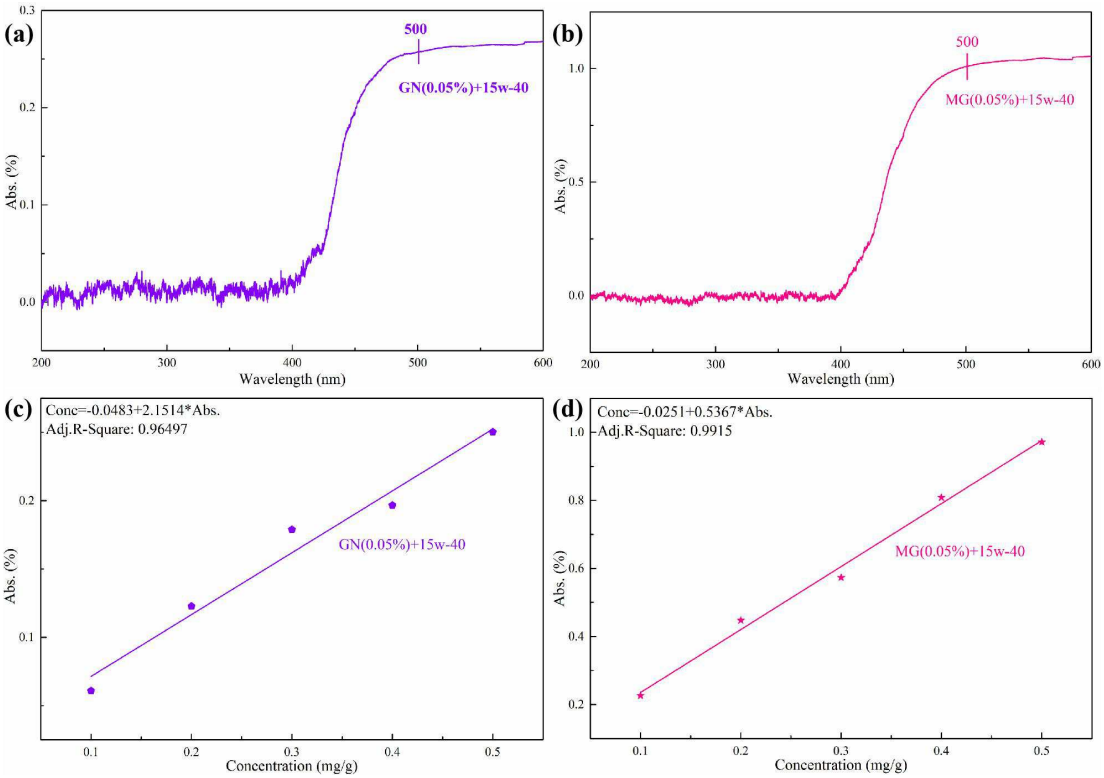

Figure 13. The wavelength diagrams (a), (b) and standard curves (c), (d) of GN(0.05%)+15w-40 and MG(0.05%)+15w-40

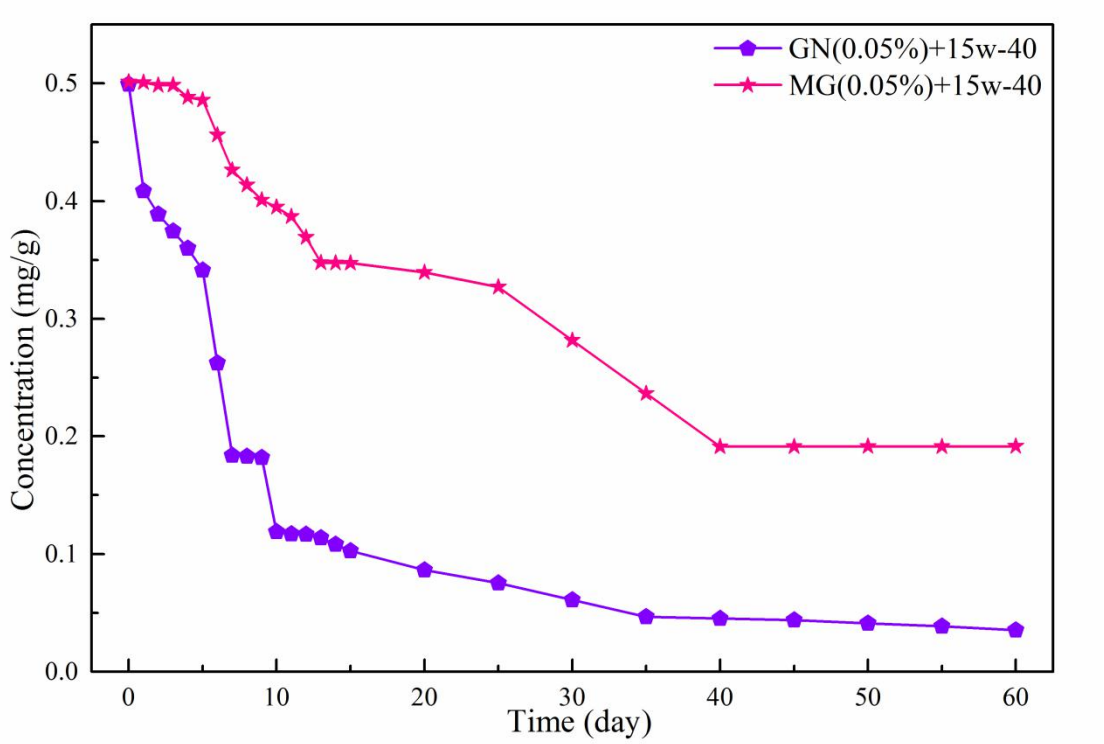

Figure 14. Concentration versus time curves of GN(0.05%)+15w-40 and MG(0.05%)+15w-40

MG has good dispersion stability in both 500N base oil and 15w-40 commercial lubricants. This phenomenon may be caused by the better effect of the carbon chain of

the PRIMENE 81-R grafted on the MG with the two lubricating oil molecules, as well as the physical and chemical properties of the lubricating oil. To explore the principle of different dispersion stabilities of MG in different base oils, we used GC-MS to analyse the molecular structure of the four base oils. Because the composition of the base oil is complicated, GC-MS analysis can only qualitatively analyse its main composition. The test results show that the main components of 500N base oil are 2,2,4-trimethylpentanediol isobutyl ester, phenylheptanone, and tris(2-chloroethyl) phosphate. Figure 15 shows the GC-MS spectrum of 500N, and Table 1 shows its main components. PAO6, Q420, and 150N were mainly composed of long-chain alkanes, and the carbon number distribution was largely C_{25}–C_{44}. Owing to the limited experimental conditions, the specific components could not be measured.

The primary component of 500N base oil is 2,2,4-trimethylpentanediol isobutyl ester (55.45%), as shown in Table 1, with multiple methyl groups. PRIMENE 81-R is a fatty primary amine with a multi-branched alkyl group in which the amino nitrogen atom is connected to the tertiary carbon atom; it has multiple branches and methyl groups. There is an interaction between methyl and methyl, known as the "magic methyl effect", that results in the steric hindrance between methyl groups being small. The steric hindrance effect, also known as the three-dimensional effect, occurs between atoms or groups in a molecule that are relatively close to each other; this causes hindrance in the spatial position between them. This is because each atom occupies a certain position in the molecular space. If the distance between the atoms is excessively small, the electrons in the atoms overlap and repel. This may make it difficult for the molecules to connect and react. Therefore, if the steric hindrance between certain atoms or groups is small, the repulsive force between them when they are close will be smaller than the repulsive force between other atoms or groups, and it is easier for them to connect. It can be concluded that a molecule with a methyl group is easily attracted to another molecule with a methyl group.

MG nanosheets have multi-branched alkyl groups of PRIMENE 81-R on the surface, so it contains multiple methyl groups. The main component of 500N base oil is 2,2,4-trimethylpentanediol isobutyl ester, which also has multiple methyl groups.

The MG nanosheets were dispersed in 500N base oil, and the steric hindrance with the surrounding 2,2,4-trimethylpentanediol isobutyl ester molecules was small, making it easier for them to connect. In this way, the MG nanosheets were stably suspended in the 500N base oil and did not agglomerate with other graphene nanosheets that were far away due to van der Waals forces. Therefore, the dispersion stability of MG in 500N base oil was greatly improved. The force between the additive molecule and the hydrocarbon solvent molecule has a significant influence on the dispersion stability of the additive in the hydrocarbon solvent.

Second, the van der Waals interaction between the methylene unit of the alkylated graphene and the hydrocarbon solvent also has a significant effect on dispersion characteristics, and this interaction increases with the increase in the methylene unit. The bonding interaction between the alkyl chain attached to the graphene nanosheets and the hydrocarbon solvent also played a greater role in monitoring the dispersion characteristics. Owing to the increase in van der Waals interactions, this cohesion increases with an increase in the number of carbon atoms in the alkyl chain, thereby improving the dispersion stability. Therefore, MG with alkyl chains is more likely to be close to hydrocarbon solvent molecules because of the presence of methyl and methylene groups. In this case, the MG nanosheets dispersed in a hydrocarbon solvent are surrounded by hydrocarbon solvent molecules, and the space between the MG nanosheets is occupied isolating them from each other. In this way, the van der Waals force and π-π effect between the MG nanosheets cannot be brought into play, and agglomeration and settlement will not occur. Because of the forces at the micromolecular level, the MG nanosheets at the macro-level exhibit excellent dispersion and stability in the 500N base oil.

The excellent dispersion of MG nanosheets in 500N base oil is also related to its physical and chemical properties. As shown in Table 2, 500N has a higher viscosity than the other three base oils. The kinematic viscosities at 100 and 40 ℃ are 11.4 and 88.5 mm^2/s, respectively. The high viscosity of the hydrocarbon solvent also leads to greater resistance between MG nanosheets that tend to agglomerate, making it difficult for them to get close. Therefore, there was no significant agglomeration, and

improved dispersion and stability were observed.

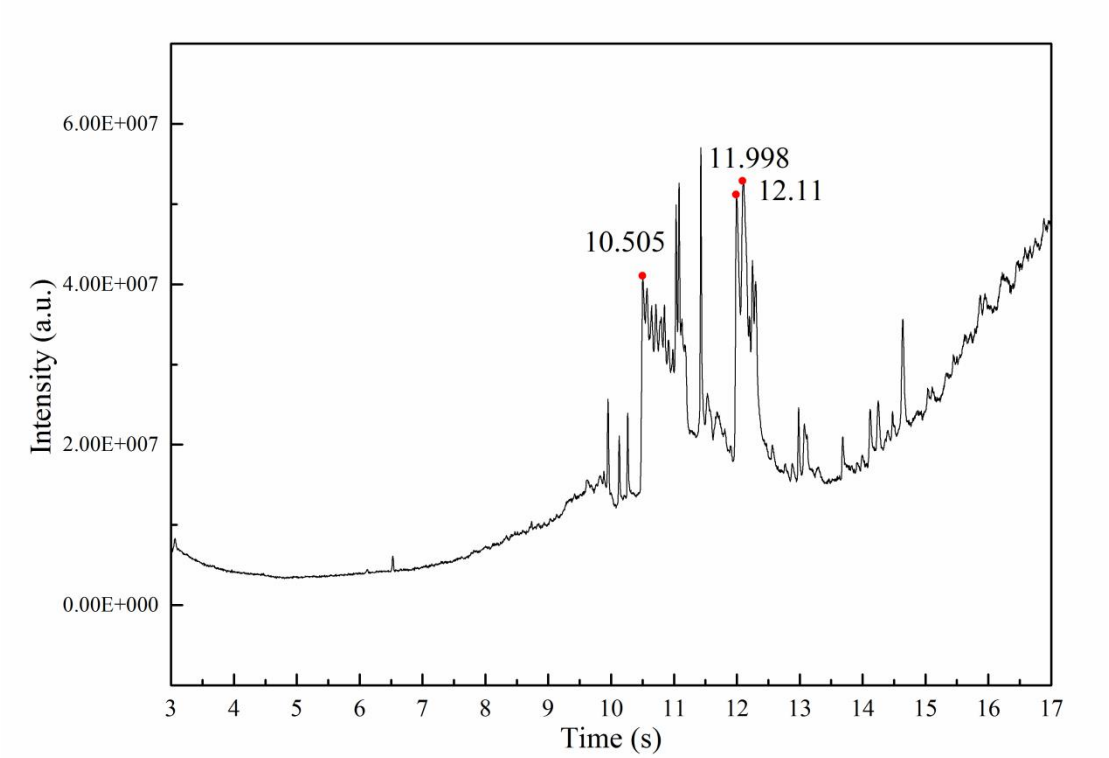

Figure 15. GC-MS spectrum of 500N base oil

Table 1. Main components of 500N base oil

Number	Time (s)	Substance	Structural formula	Concentration (%)	CAS NO
1	10.505	2,2,4-Trimethylpentanediol isobutyl ester	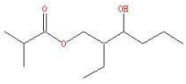	55.45	6846-50-0
2	11.998	Phenylheptanone	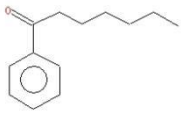	10.74	1671-75-6
3	12.11	Tris (2-chloroethyl) phosphate	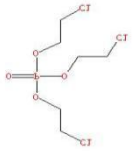	10.32	115-96-8

Table 2. Physical and chemical properties of the base oils

Oil	Relative density（15.6 ℃/g/ml）	Kinematic viscosity/（mm^2/s）		Viscosity index	Pour point/℃	Flash point (open cup)/℃	Appearance
		100℃	40℃				

500N	0.853	11.4	88.5	103	-24	256	Colourless and transparent
PAO6	0.827	5.8	31	138	-57	246	Colourless and transparent
Q420	0.816	4.08	18.29	150	-36	230	Colourless and transparent
150N	0.8372	5.014	25.46	108	-17	221	Colourless and transparent

3.3 Tribology of lubricants

In this study, a UMT-TriboLab friction and wear tester was used to evaluate the influence of several parameters (MG concentration, test load, and sliding frequency) on the tribological properties of MG lubricants. The influence of these parameters was determined by analysing the change in the average friction coefficient and wear scar diameter. A four-ball friction and wear tester was also used to conduct tribological tests on 500N base oil and 15w-40 commercial lubricants with different concentrations of MG.

3.3.1 Effect of concentration of MG on tribological properties

Tribological experiments were performed using different concentrations (0%, 0.02%, 0.03%, 0.04%, 0.05%) of MG lubricating oil, with a load of 180 N, reciprocating frequency of 5 Hz, reciprocating stroke of 6 mm, time of 20 min, and ball diameter of 6 mm. Figure 16 shows the average friction coefficient of 500N base oil with different concentrations of MG after the UMT test. It can be seen from the figure that the average friction coefficient of the base oil with MG gradually decreases. The average friction coefficient was the lowest at an MG content of 0.03%; as the concentration increased further, the friction coefficient also began to increase. This confirms that 0.03% is the ideal concentration of MG in 500N lubricating oil, and the graph also shows that the average friction coefficients of the lubricating oil are approximately equal when 0.02% and 0.05% of MG is used. While adding insufficient

or excessive MG can result in the same coefficient of friction, the form of friction may be different. Large amounts of MG may cause abrasive wear, and not enough causes adhesive wear owing to the unstable rupture of the oil film. Therefore, when anti-friction and anti-wear materials are used as lubricating oil additives, the optimal addition amount is very important. Figure 17 shows the average wear scar width under the UMT test of 500N base oil with different concentrations of MG. The figure shows that the change in the average wear scar width is consistent with the average friction coefficient; when 0.03% of MG was added, the average wear scar width was the smallest, with an increase in width when the concentration increased or decreased. This shows that under the UMT friction test, the 500N base oil with MG nanosheets had both anti-friction and anti-wear effects.

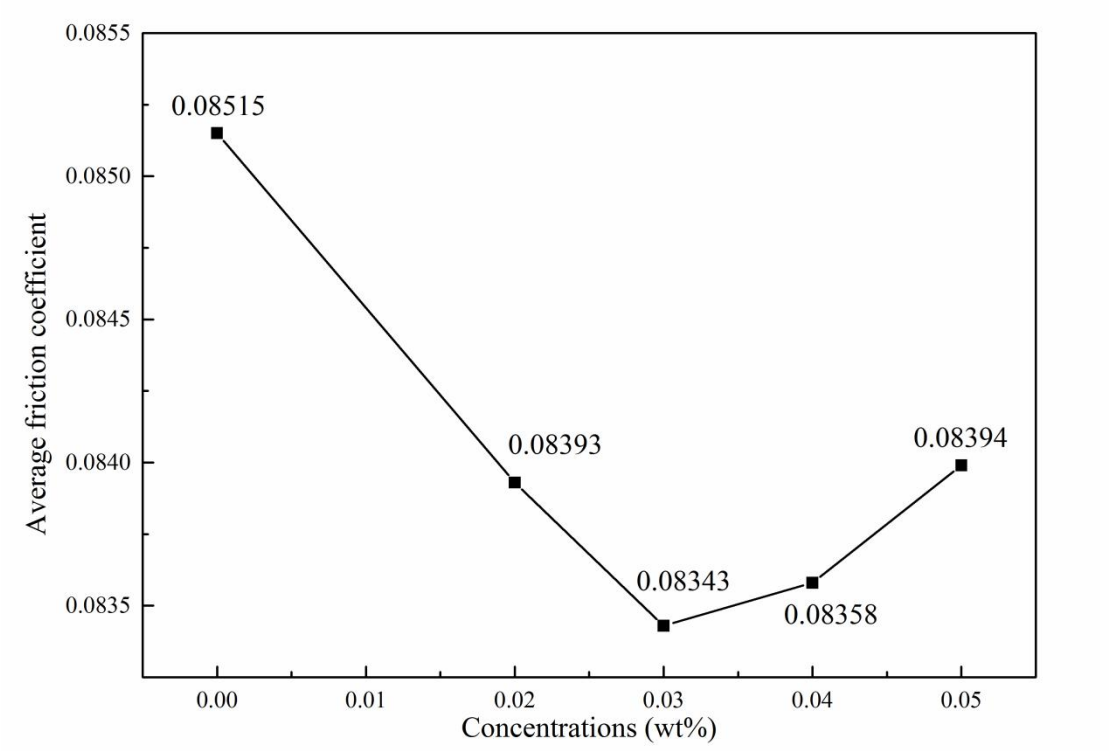

Figure 16. Average friction coefficients of 500N with different concentrations of MG under UMT tests

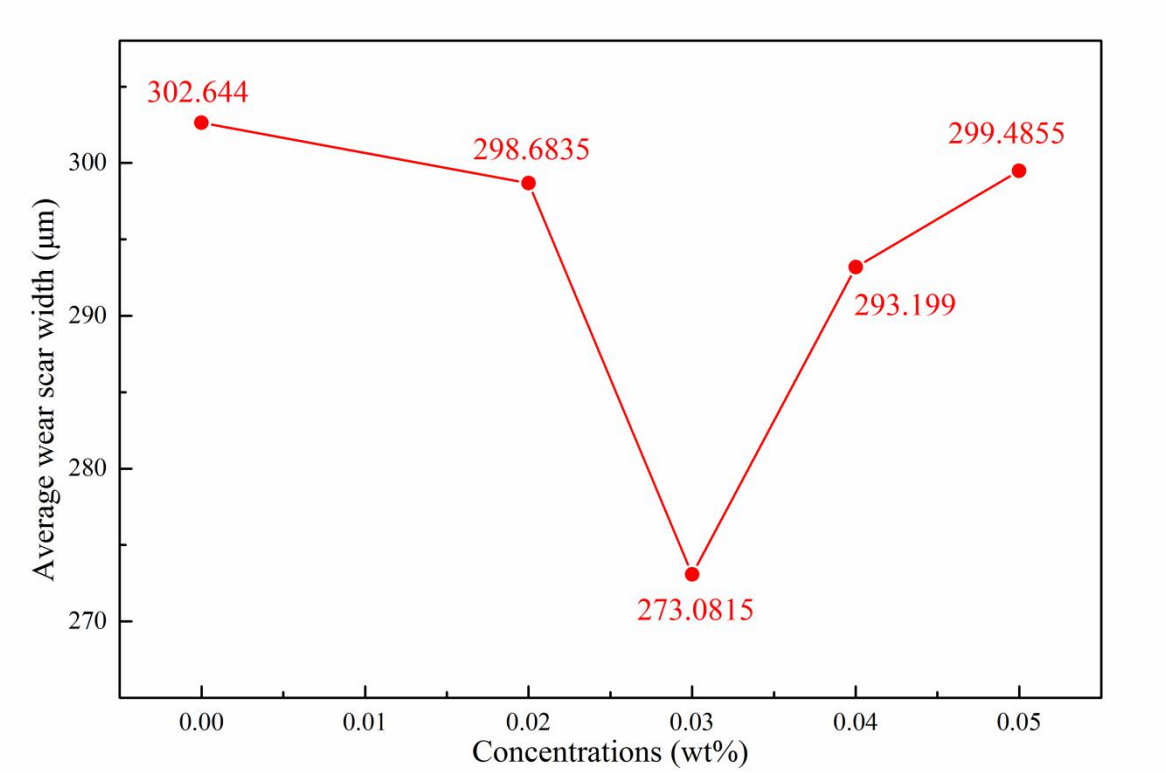

Figure 17. Average wear scar widths using 500N with different concentrations of MG under UMT tests

3.3.2 Effect of applied load on tribological properties

According to the results of the above friction test, 0.03% is the ideal MG content in 500N base oil. Therefore, UMT friction tests with different loads were performed on 500N base oil with 0.03% MG. Five different loads (50, 100, 150, 180, 230 N) were tested with a reciprocating frequency of 5 Hz. The reciprocating stroke, time, and ball diameter were unchanged. Figure 18 (a) and (b) shows the average friction coefficient and average wear scar width under different loads. From these figures, when the load is increased from 50 to 100 N, the friction coefficient of the lubricating oil decreases, and the wear scar width increases. When the load is 50 N, the higher friction coefficient may be due to the internal friction of the lubricating oil itself. After the load increased, the internal friction was transformed into sliding friction on the contact area. At a load of 100 N, the lubricating oil may form an oil film on the friction contact area after being squeezed to protect the friction contact surface. In addition, the larger the wear scar, the smaller the contact stress and the relative reduction in the friction coefficient. However, when the load was increased to 150 N,

the friction coefficient began to increase again, and the width of the wear scar increased. At this time, owing to the increase in contact stress during the friction process, the oil film may have been broken, and the friction contact area may have been worn. When the load continued to increase to 180 N, the friction coefficient decreased again, and the wear scar width reduced. We believe that the MG in the friction contact area formed a physically deposited film, and possibly a chemical reaction film, protecting the friction contact interface. When the load increased to 230 N, the coefficient of friction began to rise again, and the width of the wear scar increased significantly. Because the contact stress is large, the friction film in the contact area begins to rupture, the metal surface is abraded, and the wear spots become significantly larger. The overall results show that as the load gradually increases, the wear scar size gradually increases, and the friction coefficient is affected by many factors. When the load was 180 N, the friction coefficient was minimised.

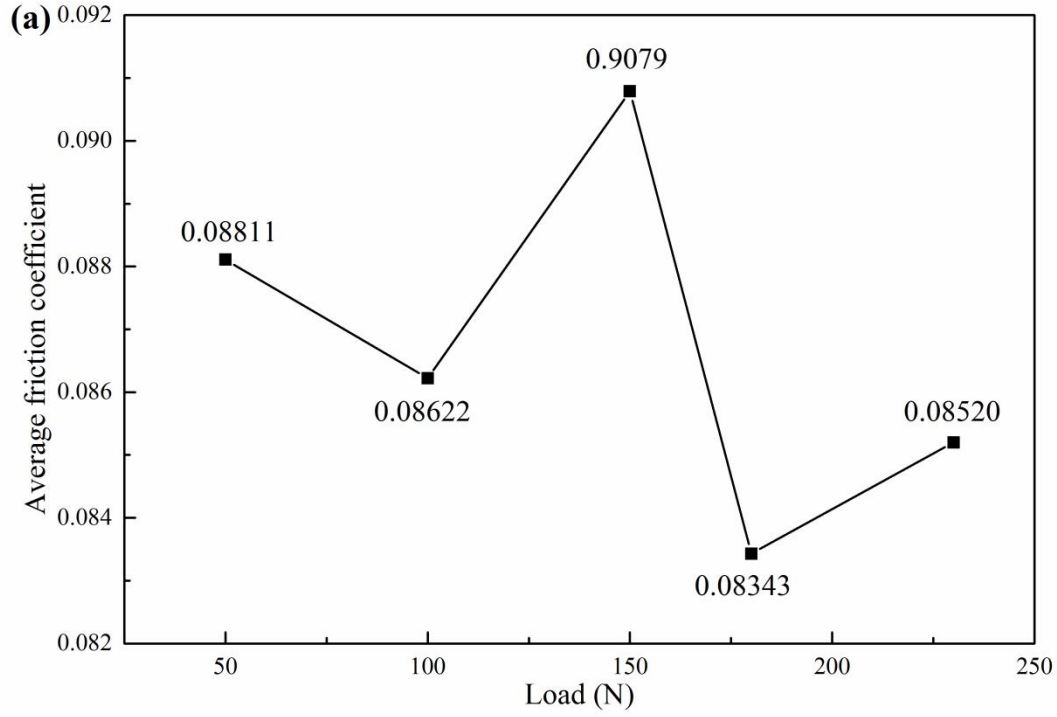

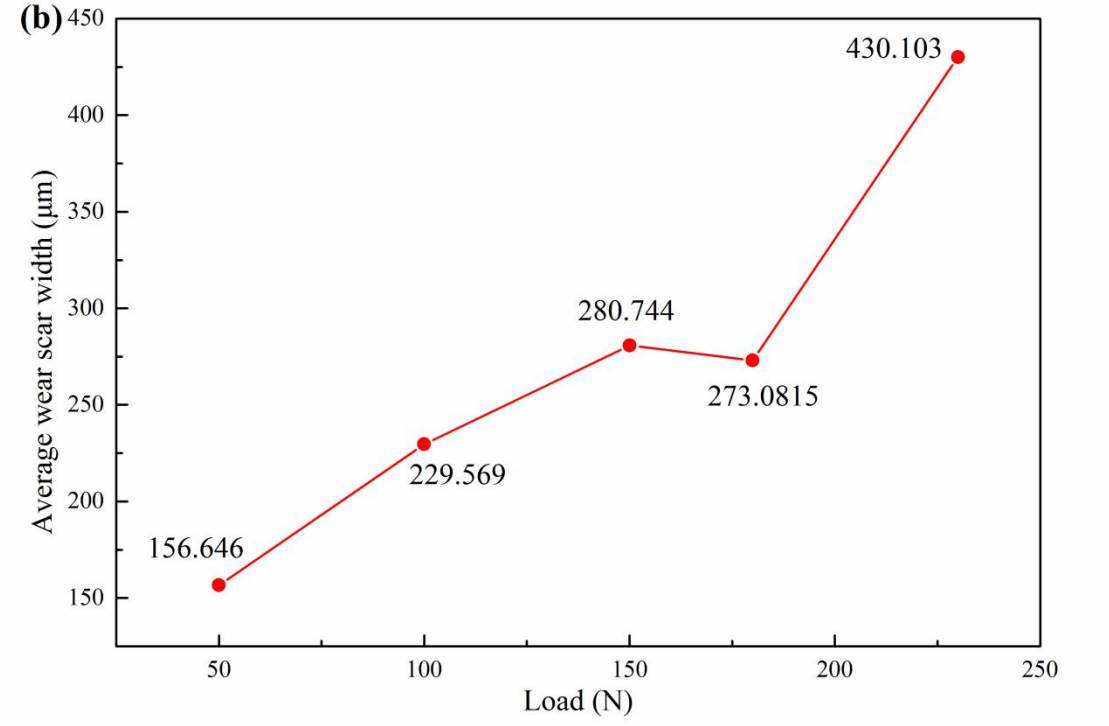

Figure 18. Average (a) friction coefficients and (b) wear scar widths of 500N with 0.03% MG added after UMT tests under different loads

3.3.3 Effect of sliding frequency on tribological properties

According to the results of the above friction test, the optimal conditions were 0.03% MG in 500N base oil with a load of 180 N; therefore UMT friction tests with different reciprocating frequencies (1, 3, 5, 7, 9 Hz) were carried out under these conditions. The reciprocating stroke, time, and ball diameter were the same as those used previously. Figure 19 (a) and (b) show the average friction coefficient and average wear scar width obtained during the UMT tests. From Figure 19 (a) and (b), as the frequency increases, the friction coefficient continues to decrease, while the wear scar width first stabilises, then increases. When the frequency increased from 1 to 5 Hz, the friction coefficient continued to decrease, and the change in the wear scar width was minimal and relatively stable. This change may be because as the friction frequency increases, an MG physical deposition film forms on the contact area. The increase in friction temperature may cause the formation of a chemical reaction film on the metal surface, which also protects the friction contact interface and reduces friction and wear. When the frequency continues to increase to 7 and 9 Hz, the friction

coefficient continues to decrease, but the wear scar width increases significantly. Therefore, the decrease in the friction coefficient is largely caused by the increase in the size of the wear scar and the decrease in the contact stress. This may be because the high frequency caused the friction film to rupture and the degree of wear to increase. The overall results show that at a frequency of 5 Hz, the tribological properties of the lubricating oil improve significantly, and the friction coefficient is reduced, but the size of the wear scar remains basically unchanged. The physical deposition and chemical reaction films work together to hinder the direct contact of the metal surfaces, exhibiting anti-friction and anti-wear effects.

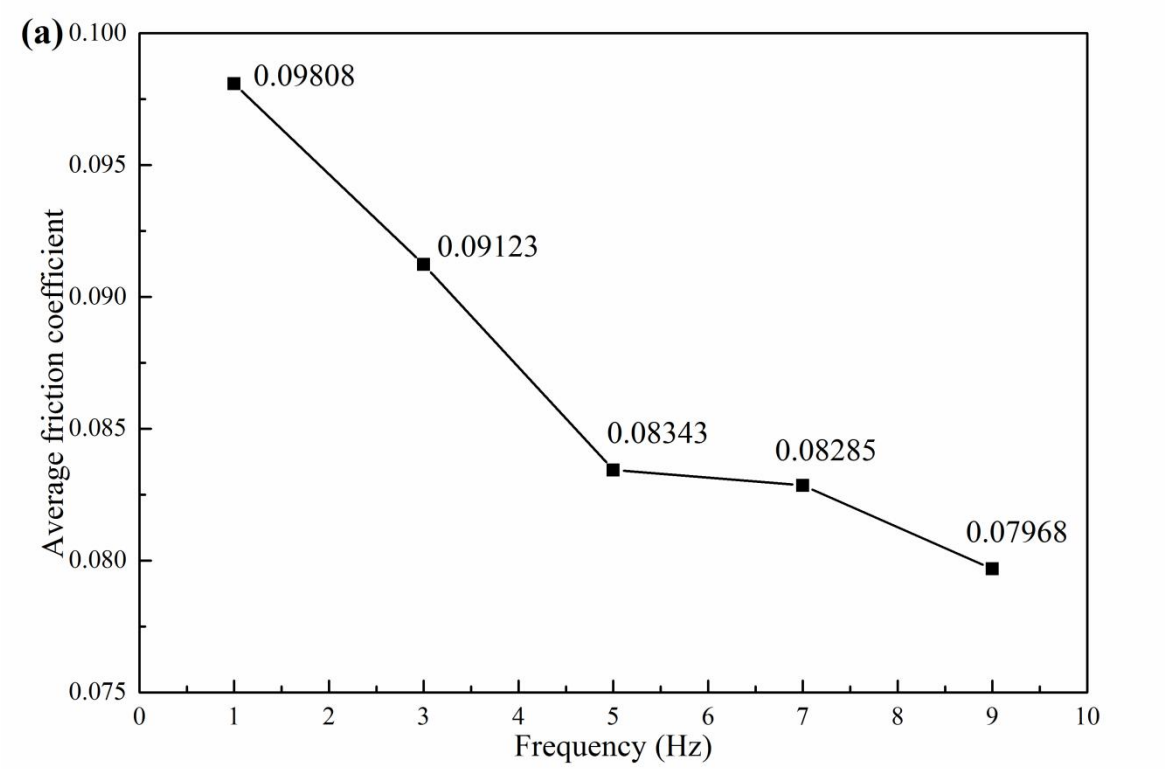

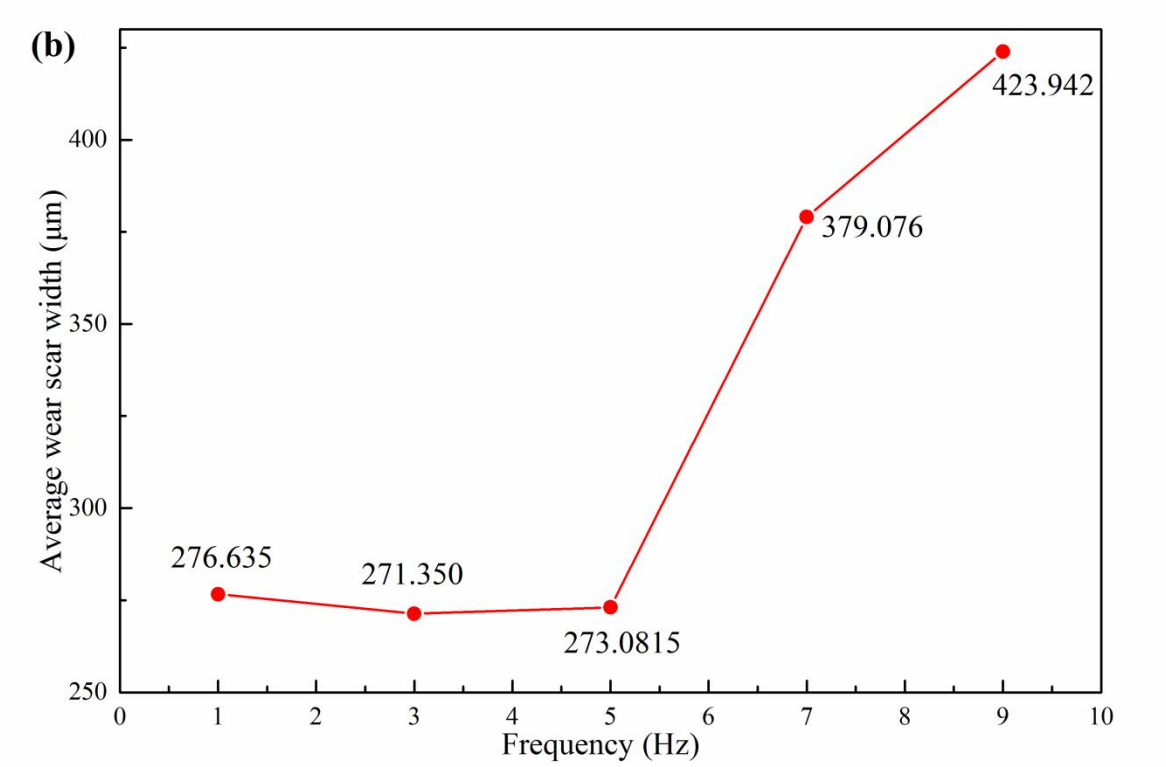

Figure 19. Average (a) friction coefficients and (b) wear scar widths (b) of 500N with 0.03% MG after UMT tests under different frequencies

3.3.4 Four-ball friction and wear test

A four-ball friction and wear test was performed on 500N base oil with different concentrations of MG. The experimental conditions were a load of 392 N, rotation speed of 1200 r/min, time of 30 min, and temperature of 25 °C. The friction coefficient of 500N base oil with MG concentrations of 0%, 0.02%, 0.03%, 0.04%, 0.05% over time are shown in Figure 20. From the figure, the friction coefficient of all lubricating oils increased significantly at the beginning of the experiment, before gradually decreasing and stabilising. The increase in the friction coefficient in the early stage increases the friction contact point wear scars, the contact area becomes larger, the contact stress becomes smaller, and the friction coefficient gradually decreases to a stable state. The pure 500N exhibited the largest friction coefficient among the lubricants. This was followed by MG(0.05%)+500N, MG(0.02%)+500N, and MG(0.04%)+500N. MG (0.03%)+500N had the lowest friction coefficient, although its early value was relatively low, while its later value was similar to that of

MG(0.02%)+500N and MG(0.04%)+500N.

The change in the friction coefficient for each sample is not clear from Figure 20. Therefore, the average friction coefficients of the lubricants were analysed, as shown in Figure 21. The change in the average friction coefficient of lubricating oil with MG concentration has a U-shaped profile. The average friction coefficient of the pure base oil was the largest, decreasing gradually at MG concentrations of 0.02% and 0.03% and increasing with 0.04% and 0.05% MG. Although the average friction coefficient began to increase after the concentration increased, it was still lower than the average friction coefficient of the pure base oil. This also shows that, with the addition of an appropriate amount of MG, the anti-friction properties of lubricating oil improve. The lowest average friction coefficient was obtained with a 0.03% MG concentration, further confirming that 0.03% is the optimal MG concentration in 500N base oil.

This conclusion is consistent with the results of the average wear scar diameter of the five lubricants (Figure 22). When the concentration of MG was 0.03%, the average wear scar diameter was the lowest among the lubricants. Moreover, the change in the average wear scar diameter of the five lubricants is similar to the change in the average friction coefficient, with a curve that drops and rises. The overall results show that within a certain concentration range, the addition of MG can significantly improve the anti-friction and anti-wear performance of 500N base oil. In addition, 0.03% is the optimal amount of MG added to 500N base oil. This conclusion is consistent with that found from UMT testing.

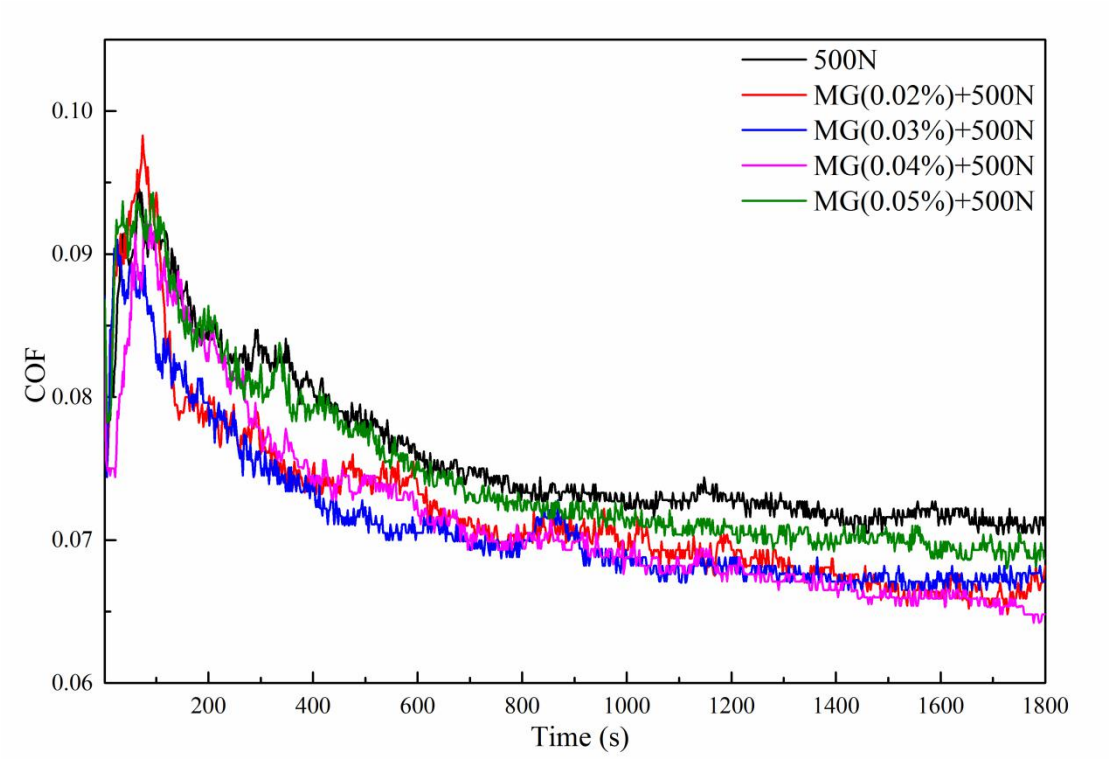

Figure 20. Friction coefficient curves of 500N base oil with various concentrations of MG during four-ball tests

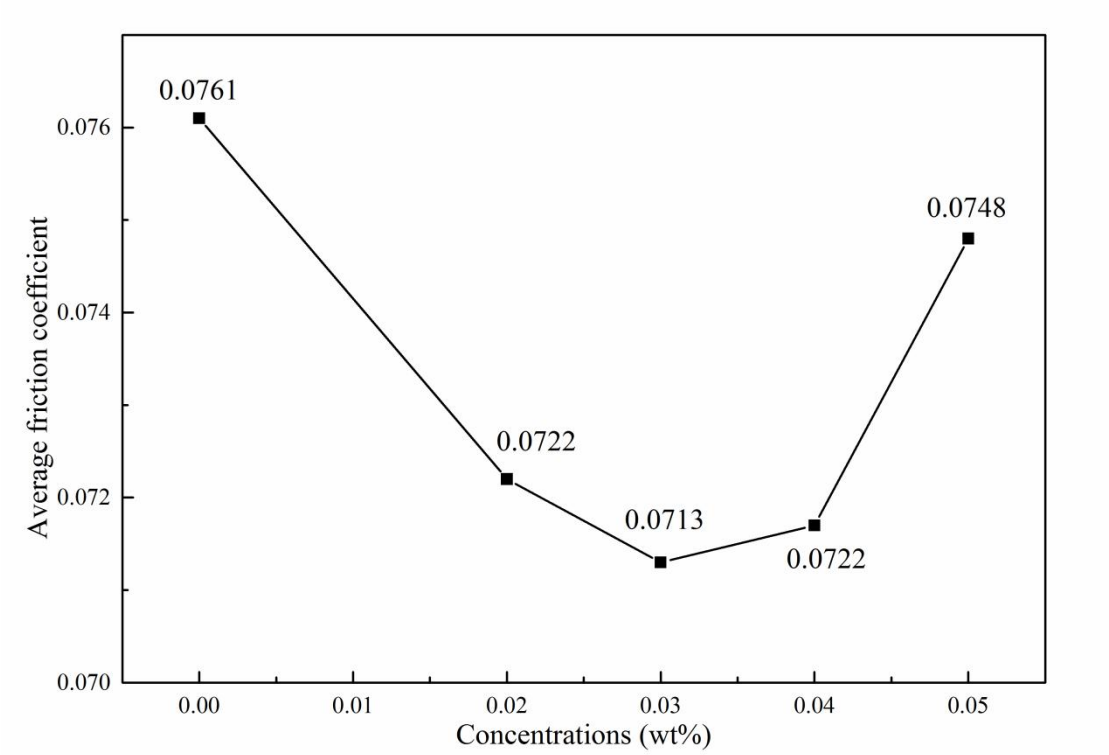

Figure 21. Average friction coefficients of 500N base oil with various concentrations of MG under four-ball tests

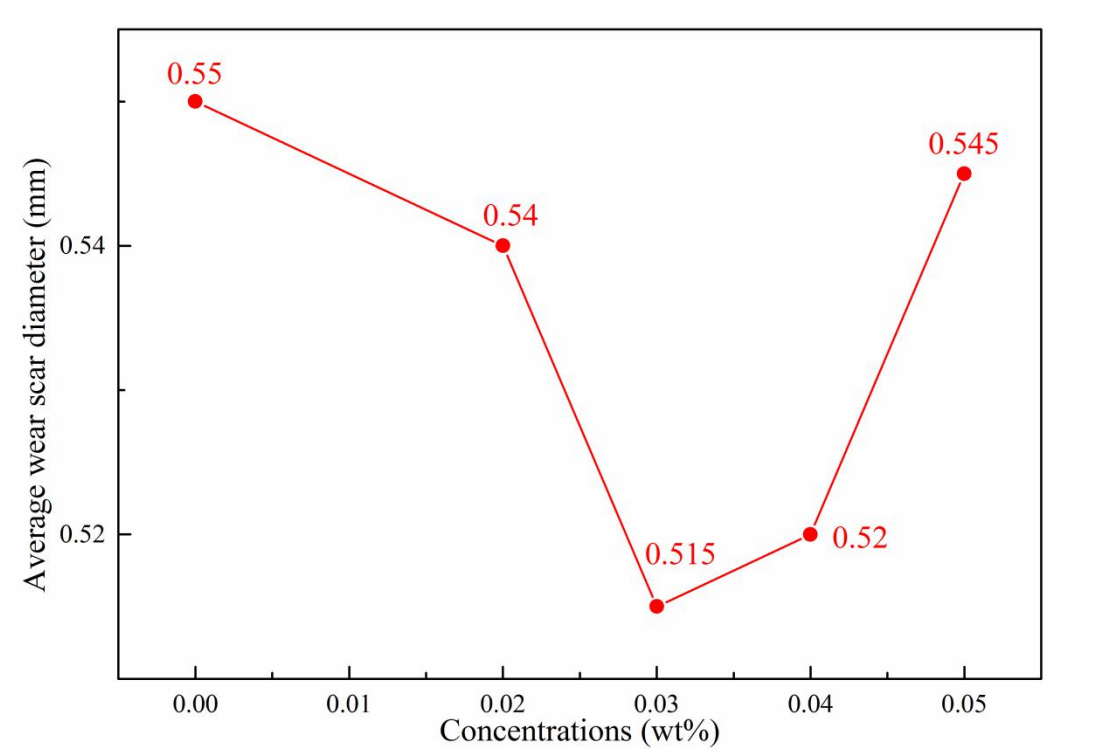

Figure 22. Average wear scar diameters of 500N base oil with various concentrations of MG under four-ball tests

Next, a four-ball friction and wear test was performed using pure 15w-40 commercial lubricant and 15w-40 commercial lubricant with 0.02% MG. The experimental conditions were a load of 392 N, speed of 1200 r/min, time of 60 min, and temperature of 25 °C. Figure 23 shows the time-varying curve of the friction coefficient of pure 15w-40 and 15w-40 with MG. The friction coefficient of 15w-40 with MG is significantly lower than that of pure 15w-40, and the friction coefficient changes more smoothly. Except for a slight increase in the early stage, the friction coefficient was very stable, with no significant fluctuation in the later stage. This phenomenon occurs because a stable oil film is formed on the friction surface, preventing direct contact with the friction surface. However, the friction coefficient of pure 15w-40 exhibited a relatively large change, with distinct fluctuations. The friction coefficient increased significantly at approximately 20 min, and fluctuations occurred at approximately 40 min. This drastic change in the friction coefficient is caused by the unstable oil film on the friction surface, and the continuous rupture during the friction process, allowing for direct contact with the metal surface.

Figure 24 shows the average friction coefficient and average wear scar diameter of pure 15w-40 and 15w-40 with MG. The average friction coefficients of pure and MG-containing 15w-40 were 0.0970 and 0.0771, respectively, which is a reduction of 20.5% from the addition of MG. The wear scar diameters of pure and MG-containing 15w-40 were 0.56 and 0.33 mm, respectively, which is a 41.1% reduction. This shows that MG improves the anti-friction and anti-wear properties of 15w-40. From the results in Section 3.2, the stable concentration of MG in 15w-40 lubricating oil is 0.02 mg/g, that is, a mass fraction is 0.02%. Therefore, this concentration was used for the friction performance test. In general, adding MG to 15w-40 lubricating oil at a ratio of 0.02% can not only stably disperse the MG, but also improve the anti-friction and anti-wear properties of the oil.

No matter added to 500N base oil or 15w-40 commercial lubricating oil, no matter in four ball friction test or UMT friction test, Mg can greatly improve the friction reduction and wear resistance of lubricating oil.And MG has excellent dispersion stability in lubricating oil, which means that MG can exert its excellent characteristics for a long time, so that the lubricating oil has a lasting anti-friction and anti-wear effect. This is the ultimate goal of our research, to prepare modified graphene lubricants that can have anti-friction and anti-wear properties for a long time.

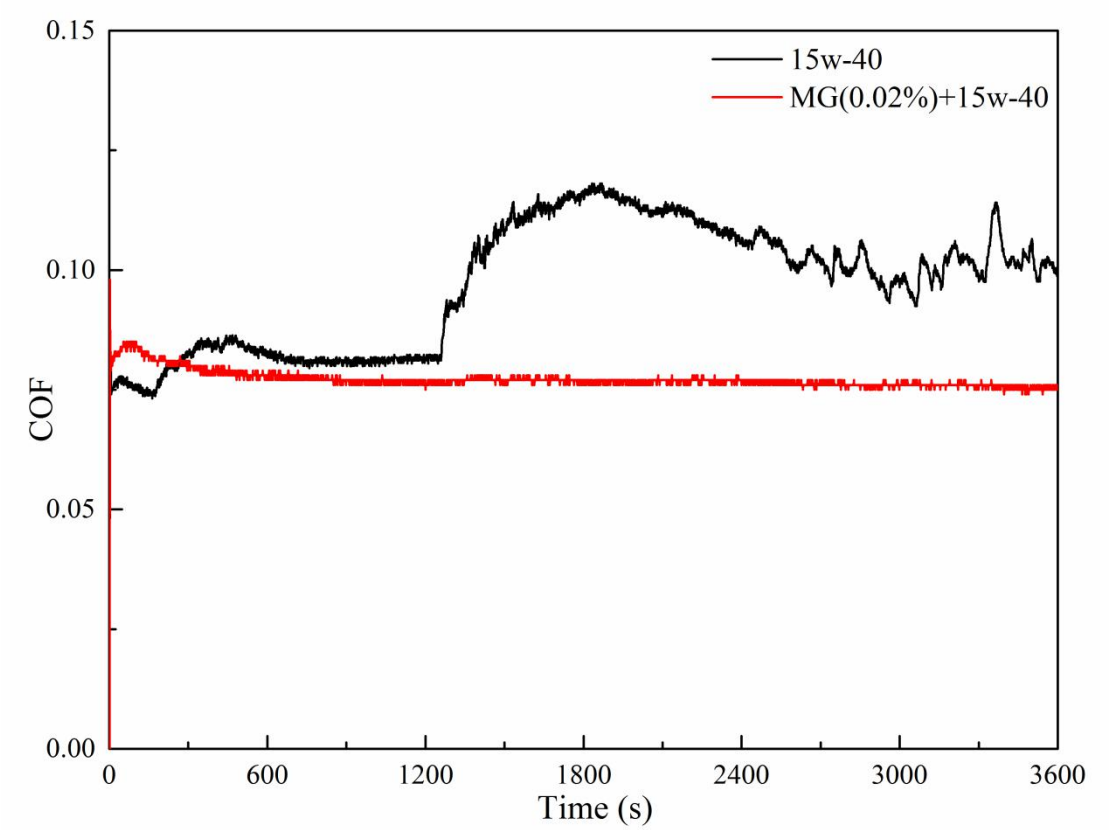

Figure 23. Friction coefficient curves of pure 15w-40 and 15w-40 with 0.02% MG under four-ball tests

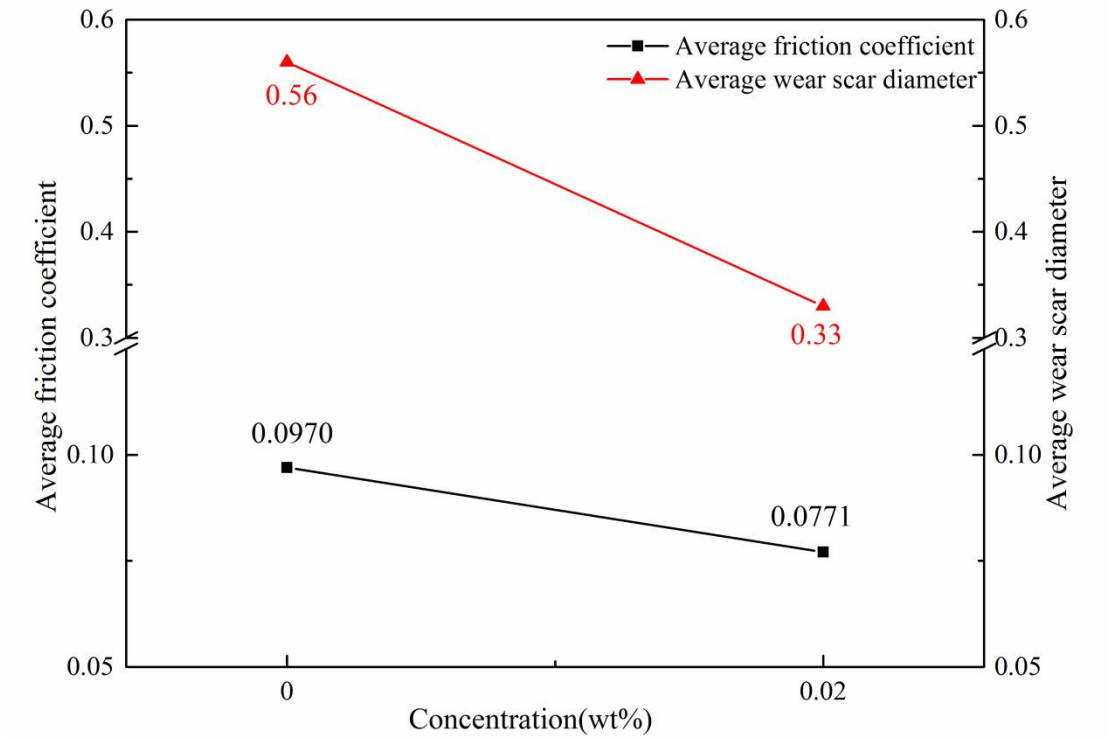

Figure 24. Average friction coefficients and average wear scar diameters of pure 15w-40 and 15w-40 with 0.02% MG under four-ball tests

3.4 Post-tribology characterization of wear tracks

A white light interferometer was used to observe the wear morphology of the steel block surface after the UMT test with pure 500N and 500N with 0.03% MG, as shown in Figure 25(a) and (b). Figure 25(a) shows the wear surface of the steel plate after the UMT test under pure 500N lubrication. Distinct strip-shaped wear scars were observed. In the x-direction cross-sectional view, we can see that there is a large, recessed area in the centre that represents the depth of the wear scars. Figure 25(b) shows the wear scar under the lubrication of 500N base oil with 0.03% MG; there are no distinct traces, the worn and unworn areas are not significantly different, and the wear area of the x-direction cross-sectional view does not change. This also shows that MG improves that anti-wear properties of 500N because the lubricating oil with added MG can form a friction film on the surface of the steel block during the friction process, preventing friction surface contact and effectively reducing the amount of wear.

(a) 500N

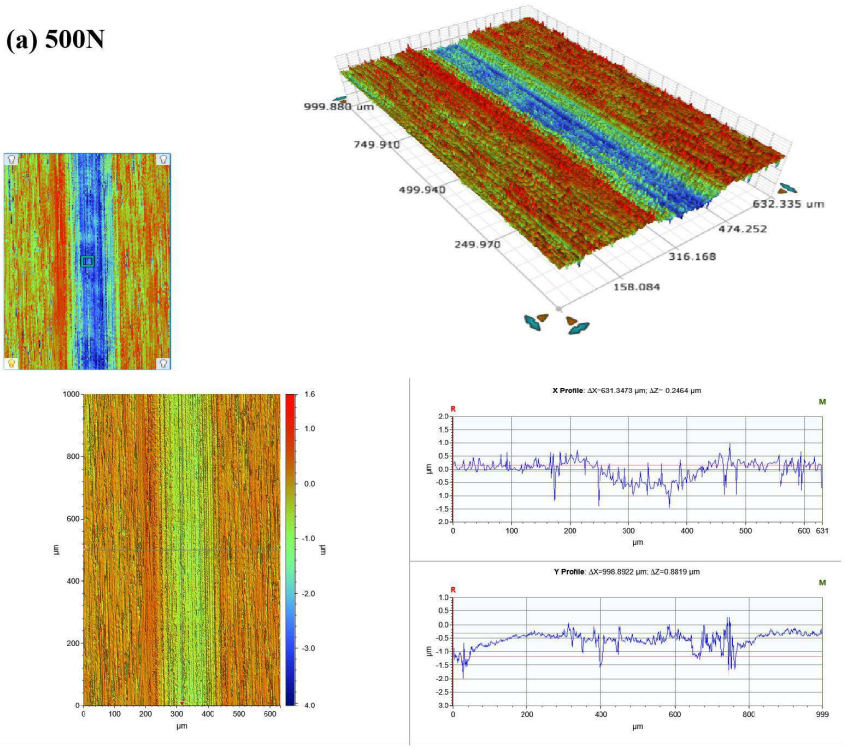

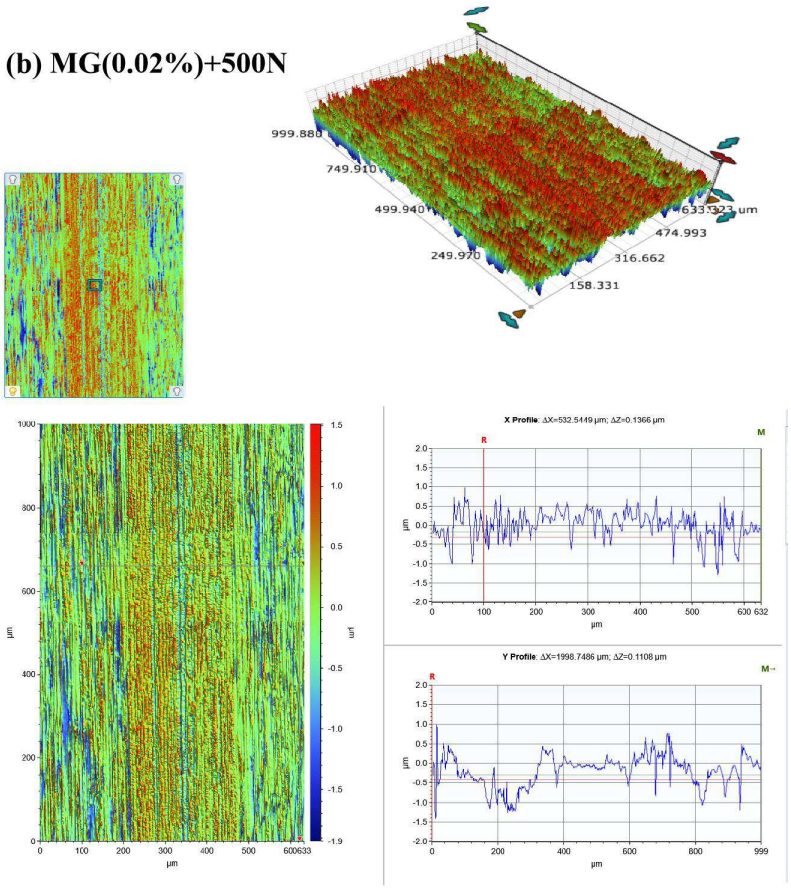

Figure 25. Wear morphologies of steel block surfaces after UMT testing under the lubrication of (a) pure 500N and (b) 500N with 0.03% MG

Raman spectroscopy was performed on the wear surface of the steel block after the UMT friction test, and the presence of substances on the surface was analysed. Figure 26 shows the Raman spectra of the worn steel block surfaces after the UMT friction test lubricated by pure 500N base oil and 0.03% MG 500N base oil. It can be seen from the figure that when the Raman displacement is approximately 640 cm^{-1}, diffraction peaks appear on the wear surface of both blocks, indicating the presence of Fe-containing oxides, such as Fe_2O_3 and FeO. This shows that during the friction test, oxidation reactions occurred between the lubricating oils and the metal surface, generating oxidation products to protect the friction contact interface. It is noticeable that the Raman diffraction peak intensity of Fe oxides on the wear surface under the lubrication of pure 500N is relatively low. This indicates that the oxidation reaction that occurs during the friction process is not violent, less Fe oxides are generated, and the friction surface is not effectively protected. Therefore, friction and wear reduction

rely on the oil film formed on the surface of the base oil. The analysis in Figure 26 shows that the typical D and G peaks of graphene are detected on the wear surface lubricated with 0.03% MG 500N, while the surface lubricated with pure base oil does not have these distinct peaks. This result shows that an orderly and stable graphene protective film is formed on the wear surface during the UMT friction test, and it can be stably adsorbed on the friction surface, preventing direct contact of the friction surfaces, and repairing and polishing the rough surface, effectively reducing friction and wear. In general, the lubricating oil with added MG generates oxides on the contact surface during the friction process to form a chemical reaction film, which protects the worn surface; in addition, it forms an orderly and stable graphene physical deposition film to reduce the direct contact with the friction surface, reducing friction and wear.

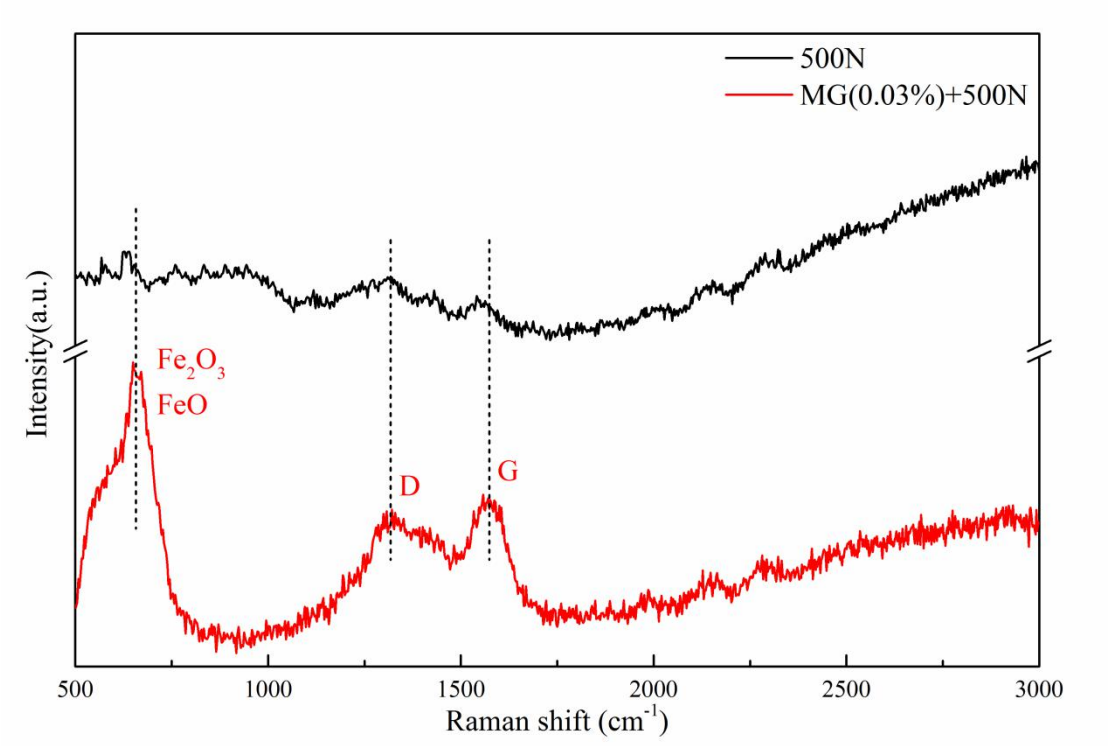

Figure 26. Raman spectra of the surface of the worn steel block after UMT friction tests using pure 500N and 500N with 0.03% MG

4. Conclusion

Graphene has excellent anti-friction and anti-wear properties, but it agglomerates easily and is difficult to stably disperse in hydrocarbon solvents, which is the main reason it is difficult to realise excellent long-term performance when using graphene

as a lubricant additive. To solve this problem, graphene was covalently modified in this study. We used a mild oxidation method to selectively graft carboxyl groups on the edge of the graphene sheet and coupled it with PRIMENE 81-R to prepare a covalently MG. MG was characterised by FT-IR, XPS, Raman spectroscopy, XRD, SEM, and other material analysis methods. The results of in-depth dispersion stability studies have shown that the grafted alkyl chains of the MG sheet layer exhibit excellent stable dispersion in 500N base oil and 15w-40 commercial lubricants, with a stability of over 2 months, which is essential for achieving efficient tribological performance. MG was used as a friction-reducing and anti-wear additive for 500N base oil and 15w-40 commercial lubricating oil, and its tribological performance was evaluated using two friction contact forms: steel ball-steel ball and steel ball-steel plate. The friction test results show that by dispersing a small amount of MG in the lubricating oil, the anti-friction and anti-wear performance of the oil to the steel-steel friction pair can be improved. Through the detection and analysis of the worn surface, it was found that a chemical reaction film and an orderly graphene physical deposition film were formed on the contact surface during the friction process, which protected the worn surface and reduced their direct contact, thereby reducing friction and wear. This provides a useful reference for the design and optimisation of the application of MG materials in tribology and has the potential to reduce industrial energy consumption and expand the application of graphene materials for lubrication.

Compliance with Ethical Standards

- The authors declare that they have no known competing financial interests or personal relationships that could have appeared to influence the work reported in this paper.
- The authors declare that this paper does not involve human participants and/or animal research.
- The authors have informed consent to the submission of this paper

Acknowledgement

This research was funded by the National Natural Science Foundation of China (grant number 12062002), Natural Science Foundation of Guangxi Province of China

(grant number 2018GXNSFAA138174). We would like to thank Editage (www.editage.cn) for English language editing.

References

[1] Nair RR, Blake P, Grigorenko AN, Novoselov KS, Booth TJ, Stauber T, et al. Fine Structure Constant Defines Visual Transparency of Graphene. Science 2008;320(5881):1308.

[2] Chae HK, Siberio-Pérez DY, Kim J, Go Y, Eddaoudi M, Matzger AJ, et al. A route to high surface area, porosity and inclusion of large molecules in crystals. Nature 2004;427(6974):523–527.

[3] Allen MJ, Tung VC, Kaner RB. Honeycomb Carbon: A Review of Graphene. Chem Rev 2010;110(1):132–145.

[4] Bouša D, Pumera M, Sedmidubský D, Šturala J, Luxa J, Mazanek V, et al. Fine tuning of graphene properties by modification with aryl halogens. Nanoscale 2016;8(3):1493–1502.

[5] Sadasivuni KK, Ponnamma D, Thomas S, Grohens Y. Evolution from graphite to graphene elastomer composites. Prog Polym Sci 2014;39(4):749–780.

[6] Balandin AA, Ghosh S, Bao W, Calizo I, Teweldebrhan D, Miao F, et al. Superior Thermal Conductivity of Single-Layer Graphene. Nano Lett 2008;8(3):902–907.

[7] Lee CG, Li Q Y, Kalb W, Liu XZ, Berger H, Carpick RW et al. Frictional Characteristics of Atomically Thin Sheets. Science 2010;328(5974):76–80.

[8] Kong LJ, Zhou XY, Fan SY, Zaijun L, Zhiguo G. Study on the Synthesis and Electrochemical Performance of Histidine-Functionalized Graphene Quantum Dots@Silicon Composite Anode Material. Acta Chim Sinica, 2016;74(7):620.

[9] Ambrosi A, Bonanni A, Sofer Z, Cross JS, Pumera M. Electrochemistry at Chemically Modified Graphenes. Chem Eur J 2011;17(38):10763–10770.

[10] Zhang YB, Tang T, Girit C, Hao Z, Martin MC, Zettl A, et al. Direct observation of a widely tunable bandgap in bilayer graphene. Nature 2009;459(7248):820–823.

[11] Zhao J, Mao J, Li Y, He Y, Luo J. Friction-induced nano-structural evolution of graphene as a lubrication additive. Appl Surf Sci 2018;434:21–27.

[12] Restuccia P, Righi MC. Tribochemistry of graphene on iron and its possible role in lubrication of steel. Carbon 2016;106:118–124.

[13] Xu YF, Peng YB, You T, Yao L, Geng J, Dearn KD, et al. Nano-MoS^2 and Graphene Additives in Oil for Tribological Applications. In: Saleh, TA, editors. Nanotechnology in Oil and Gas Industries, Cham: Springer; 2018, p. 151–191.

[14] Liang H, Bu Y, Zhang J, Cao Z, Liang A. Graphene Oxide Film as Solid Lubricant. ACS Appl Mater Interfaces 2013;5(13):6369–6375.

[15] Meng Y, Su F, Chen Y. Supercritical Fluid Synthesis and Tribological Applications of Silver Nanoparticle-decorated Graphene in Engine Oil Nanofluid. Sci Rep 2016;6(1):1–12.

[16] Qiao Y, Zhao H, Zang Y, Zhang Q and Liu H. Research progress of functionalization modification and applications of graphene as lubricating additive. Chem. Ind. Eng. Prog 2014; Z1 216–23.

[17] Georgakilas V, Tiwari JN, Kemp KC, Perman JA, Bourlinos AB, Kim KS, et al. Noncovalent Functionalization of Graphene and Graphene Oxide for Energy Materials, Biosensing, Catalytic, and Biomedical Applications. Chem Rev 2016;116(9):5464–5519.

[18] Wajid AS, Das S, Irin F, Ahmed HT, Shelburne JL, Parviz D, et al. Polymer-stabilized graphene

dispersions at high concentrations in organic solvents for composite production. Carbon 2012;50(2):526–534.
[19] Zacharia R, Ulbricht H, Hertel T. Interlayer cohesive energy of graphite from thermal desorption of polyaromatic hydrocarbons. Phys Rev B 2004;69(15):155406
[20] Lee K, Hwang Y, Cheong S, Kwon L, Kim S, Lee J. Performance evaluation of nano-lubricants of fullerene nanoparticles in refrigeration mineral oil. Curr Appl Phys, 2009;9(2):e128–e131.
[21] Li D, Muller MB, Gilje S, Kaner RB, Wallace GG. Processable aqueous dispersions of graphene nanosheets. Nat Nanotechnol 2008;3(2):101–105.
[22] Si Y C, Samulski E T. Synthesis of Water Soluble Graphene. Nano Lett 2008;8(6):1679–1682.
[23] Karlický F, Kumara Ramanatha Datta K, Otyepka M, Zboril R. Halogenated Graphenes: Rapidly Growing Family of Graphene Derivatives. ACS Nano, 2013;7(8):6434–6464.
[24] Quintana M, Vazquez E, Prato M. Organic Functionalization of Graphene in Dispersions. Acc Chem Res, 2012;46(1):138–148.
[25] Englert J M, Dotzer C, Yang G, Schmid M, Papp C, Gottfried JM, et al. Covalent bulk functionalization of graphene. Nat Chem 2011;3(4):279–286.
[26] Di Pietro P, Forte G, Snyders R, et al. Sulphur functionalizion of graphene oxide by radiofrequency plasma[J]. Plasma Process Polym, 2020;17(8):2000039.
[27] Choudhary S, Mungse HP, Khatri OP. Dispersion of alkylated graphene in organic solvents and its potential for lubrication applications. J Mater Chem 2012;22(39):21032.
[28] Mungse HP, Khatri OP. Chemically Functionalized Reduced Graphene Oxide as a Novel Material for Reduction of Friction and Wear. J Phys Chem C, 2014;118(26):14394–14402.
[29] Ma J, Xiao Y, Sun Y, Hu J, Wang Y. Sulfur-Doped Alkylated Graphene Oxide as High-Performance Lubricant Additive. Nanoscale Res Lett 2020;15(1):1–11.
[30] Paul G, Shit S, Hirani H, Kuila T, Murmu NC. Tribological behavior of dodecylamine functionalized graphene nanosheets dispersed engine oil nanolubricants. Tribol Int, 2019;131:605–619.
[31] Wu P, Chen X, Zhang C, Zhang J, Luo J, Zhang J. Modified graphene as novel lubricating additive with high dispersion stability in oil. Friction, 2020;9(1):143–154.
[32] Park S, An J, Jung I, Piner RD, An SJ, Li X, et al. Colloidal Suspensions of Highly Reduced Graphene Oxide in a Wide Variety of Organic Solvents. Nano Lett, 2009;9(4):1593–1597.
[33] Suk JW, Piner RD, An J, Ruoff RS. Mechanical Properties of Monolayer Graphene Oxide. ACS Nano, 2010;4(11):6557–6564.
[34] Wepasnick KA, Smith BA, Schrote KE, Wilson HK, Diegelmann SR, Fairbrother DH. Surface and structural characterization of multi-walled carbon nanotubes following different oxidative treatments. Carbon, 2011;49(1):24–36.
[35] Cai W, Piner RD, Stadermann FJ, Park S, Shaibat MA, Ishii Y, et al. Synthesis and Solid-State NMR Structural Characterization of 13C-Labeled Graphite Oxide. Science 2008;321(5897):1815–1817.